Directed chaotic transport in Hamiltonian ratchets

Holger Schanz,[1,*] Thomas Dittrich,[2] and Roland Ketzmerick[3]
[1]*Max-Planck-Institut für Strömungsforschung und Institut für Nichtlineare Dynamik der Universität Göttingen, Bunsenstraße 10, D-37073 Göttingen, Germany*
[2]*Departamento de Física, Universidad Nacional, Santafé de Bogotá, Colombia*
[3]*Institut für Theoretische Physik, Technische Universität Dresden, D-01062 Dresden, Germany*
(Received 12 August 2004; published 16 February 2005)

We present a comprehensive account of directed transport in one-dimensional Hamiltonian systems with spatial and temporal periodicity. They can be considered as Hamiltonian ratchets in the sense that ensembles of particles can show directed ballistic transport in the absence of an average force. We discuss general conditions for such directed transport like a mixed classical phase space. A sum rule is derived which connects the contributions of different phase-space components to transport. We show that regular ratchet transport can be directed against an external potential gradient while chaotic ballistic transport is restricted to unbiased systems. For quantized Hamiltonian ratchets we study transport in terms of the evolution of wave packets and derive a semiclassical expression for the distribution of level velocities which encode the quantum transport in the Floquet band spectra. We discuss the role of dynamical tunneling between transporting islands and the chaotic sea and the breakdown of transport in quantum ratchets with broken spatial periodicity.

DOI: 10.1103/PhysRevE.71.026228 PACS number(s): 05.45.Mt, 05.60.−k

I. INTRODUCTION

Hamiltonian systems with a mixed phase space remain a challenge within the field of nonlinear dynamics, both classical and quantum. This is usually attributed to the intricate, typically self-similar structure of the phase space in these systems. There exist, however, more tangible effects which also require a coexistence of regular and chaotic dynamics but no particular fine structure. A prominent example is directed transport: An elementary yet decisive consequence of a mixed phase space is the existence of distinct regions that support qualitatively different dynamics and do not communicate with each other. Directed transport may arise locally in regular components of phase space. As a consequence of a global sum rule, and in the absence of certain symmetries, it can then be conferred to the chaotic component, as we will show in this paper.

Chaotic transport in extended Hamiltonian systems is usually associated with undirected diffusion: The width of the spatial distribution Δx grows with time as some power law $(\Delta x)^2 \sim t^\alpha$ with α between 0 and 2. Only recently has it been discovered that even in the absence of a mean external gradient, chaotic diffusion in driven Hamiltonian systems can be accompanied by a directed drift. The corresponding ballistic component of transport [1] may appear surprising on first sight, since a hallmark of chaos is the decay of all correlations including an effective randomization of the velocity with time. However, this implies only that the mean velocity of a typical chaotic trajectory approaches an asymptotic value which is characteristic of the chaotic phase-space region as a whole. In the absence of additional symmetries there is no general reason requiring this asymptotic mean velocity to be zero.

In fact, as we shall argue in Sec. II, in systems with a mixed phase space a sum rule requires chaotic transport to compensate for the directed transport possibly occurring in regular phase-space regions [2,3]. An important conclusion (Sec. II E) is that the ballistic chaotic transport has nothing to do with internal structures of a chaotic phase-space component such as cantori or other partial transport barriers. All these complicated substructures leading to, for instance, Lévy walks and anomalous diffusion in Hamiltonian ratchets [1,4,5] need not be considered in detail in order to understand that ballistic transport dominates for long times.

Deterministic ballistic transport due to a dynamical restriction of trajectories to certain phase-space regions has been observed before in dissipative systems [6–8], where the phase-space volume is contracting with time. In this situation one speaks of deterministic ratchets because of the analogy to the well-known stochastic ratchets (Brownian motors) which generate directed motion from nonequilibrium noise [9–12].

Throughout this paper, we disregard dissipation. Its absence, however, renders it more difficult to achieve directed transport, since the natural time arrow determined by dissipation is lost and has to be replaced by other mechanisms breaking time-reversal invariance. On the other hand trajectories can maintain a memory of their initial velocity for an infinite time. Therefore a precise definition of a *Hamiltonian ratchet* is not completely straightforward. The mere fact that in unbiased systems directed transport can exist and survive for infinite time is trivial; just take a free particle with some nonzero initial velocity $v_0 \neq 0$. In this sense every extended Hamiltonian system would be a ratchet.

Due to velocity dispersion an ensemble of free particles will also spread ballistically, i.e., as fast as its center of mass is transported. On the other hand, as pointed out above, there exist Hamiltonian systems where transport is ballistic, but the spreading is not. They are characterized by a locking of the average velocity to a (nonzero) value which does not

*Electronic address: holger@chaos.gwdg.de

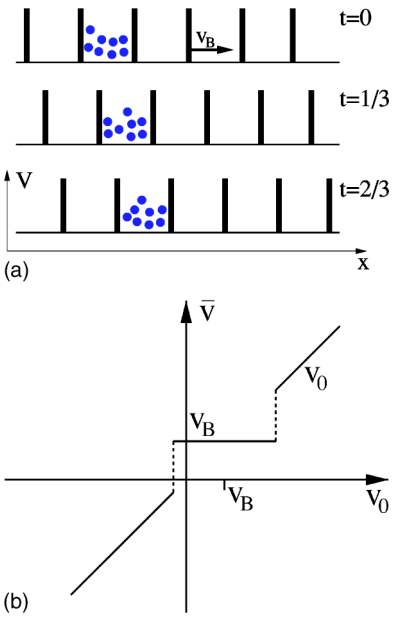

FIG. 1. (a) A trivial example for a Hamiltonian ratchet is a periodic potential that is moving at a constant velocity $v_B > 0$ such that $V(x,t) = \tilde{V}(x - v_B t)$. The system is integrable, since it is time independent in the comoving reference frame. Despite the conveyor-belt construction it is also unbiased, since the average force in a periodic potential is always zero. (b) shows the dependence of the asymptotic mean velocity $\bar{v}$ on the initial velocity v_0 under the assumption that the potential is nonzero only in negligibly small intervals. Particles with initial velocity close to v_B, namely, for $m(v_0 - v_B)^2/2 < V_{max}$, are trapped inside one well of the potential and have an asymptotic velocity $\bar{v} = v_B$ independent of the precise initial conditions.

depend on the precise initial conditions as long as they are restricted to some finite phase-space region. For the purpose of the present paper we regard this property as the definition of a Hamiltonian ratchet.

Even with this restriction it is possible to construct cases one would qualify as trivial realizations of directed transport: In the integrable system sketched in Fig. 1, for example, transport appears to be achieved by a mere change of frame. For the sake of simplicity of the definition we do not attempt to formally exclude such cases. In what follows, however, we concentrate on extended systems with a mixed phase space where one has to understand the interplay between regular and chaotic transport.

Unless symmetries of the driving potential prevent it [1], Hamiltonian ratchets as defined above lead, without average force, to a nonzero mean velocity of an ensemble of particles which were initially at rest. The same applies also to the ratchets described in [13,14], although there is no velocity locking and ensembles of particles do spread ballistically. These systems are based on a mechanism that is different from the models discussed in [1–5,15–17] and the present paper and we will not consider them here.

For Hamiltonian ratchets under the influence of an average force we show in Sec. II F that uphill regular transport is possible. In contrast, even an infinitesimal average force destroys the chaotic drift and leads to downhill acceleration.

It comes as a rather unexpected finding that Hamiltonian ratchets have applications on macroscopic, even geophysical scales where apparently friction prevails [18]. Indeed, in hydrodynamics, even in the presence of dissipation, restricting the description to position space results in a Hamiltonian form of the evolution equations if only the fluid is *incompressible*. Specifically, in geophysical applications, a periodic potential reflects the periodic boundary conditions on Earth with respect to longitude, while an asymmetry in the transverse coordinate is implied by the dependence of the Coriolis force on latitude.

Going in the opposite direction, Hamiltonian ratchets may find applications on scales where quantum effects become important. For example, in semiconductor nanostructures employed to investigate solid-state ratchets [19,20] such effects were observed. A Hamiltonian ratchet with negligible dissipation can be realized on this basis if the structure size is further decreased, such that electronic motion occurs in the ballistic regime. But this will even enhance quantum corrections.

In Ref. [3] it was concluded that quantum Hamiltonian ratchets can work if classical and quantum systems are both spatially periodic such that the quantum system has a band spectrum. Detailing our findings, we will show in Sec. III B that quantum transport relies on the semiclassical correspondence between the dynamics of wave packets and that of classical distributions in phase space: As long as a wave packet, started in the chaotic region of the phase space, say, remains predominantly restricted to this region, it will be transported with the classical mean chaotic velocity. Such quantum-classical correspondence can be attributed to the existence of different types of bands in the spectrum, with eigenfunctions concentrating semiclassically on different invariant sets of classical phase space. Since this mechanism crucially depends on classical phase-space structures, it cannot be captured using a single- (or few-)band picture. Therefore our results are not at variance with the absence of transport demonstrated within such an approximation [15,16].

However, also in the semiclassical regime, nonclassical processes like tunneling are possible which allow transitions between invariant sets of classical phase space. In Sec. III C we will address the question of why this is compatible with quantum transport unlimited in time. Only when the exact periodicity of the quantum system is destroyed do the eigenfunctions governing the long-time dynamics ignore classical phase-space structures [21] such that ratchet transport becomes a transient phenomenon. We shall deal with this case in Sec. III D.

In our conclusions (Sec. IV) we discuss in particular various ways of breaking the translation invariance of Hamiltonian ratchets and how this affects transport.

II. CLASSICAL HAMILTONIAN RATCHETS

A. The Hamiltonian of the extended system

We consider Hamiltonian systems in one dimension which are *periodic* and *unbiased* in the sense specified below. The Hamiltonian is of the form

$$H(p,x,t) = T(p) + V(x,t), \tag{1}$$

where x and p are the canonically conjugate position and momentum and $T(p)$ and $V(x,t)$ denote kinetic and potential energy, respectively.

We require that the *dynamics* be invariant under integer translations of space or time and use dimensionless variables in which both periods are unity [22], i.e., we assume the following property: For any trajectory $x(t)$ with initial conditions $x(t_0)=x_0$, $p(t_0)=p_0$ and any other trajectory $\tilde{x}(t)$ with $\tilde{x}(t_0+n)=x_0+m$, $\tilde{p}(t_0+n)=p_0$, we have $\tilde{x}(t+n)=x(t)+m$ for all t.

In the simplest case this is realized by $T(p)=p^2/2$ and a spatially and temporally periodic potential

$$V(x,t+1) = V(x+1,t) = V(x,t), \tag{2}$$

but this is not a necessary condition: If the potential contains an additional term $f(t)x$ we have $V'(x+1,t)=V'(x,t)$ only, where $V'=dV/dx$. Nevertheless, discrete translation invariance may be satisfied for the dynamics; see Sec. II F for an example.

We shall refer to the system as unbiased, if the force $-V'$ averaged over space and time vanishes,

$$\int_0^1 dx \int_0^1 dt\, V'(x,t) = 0. \tag{3}$$

In Sec. II G we will also consider systems where the kinetic energy is a periodic function of p such as $T(p)=\cos 2\pi p$ for electrons in a Bloch band. As we shall see, such systems are always unbiased.

B. The phase space of a unit cell

Instead of the extended system represented by Eq. (1), the discrete translation invariance allows us to consider an auxiliary system restricted to a single *unit cell* by imposing periodic boundary conditions at $x=1$, $t=1$. Since in this paper both representations appear in parallel, we use different symbols $\xi \equiv x \bmod 1$ and $\tau \equiv t \bmod 1$ for the cyclic variables of the unit cell.

It is a standard technique for driven systems [23] to treat time like a spatial coordinate such that a one-dimensional time-dependent system is mapped to a formally time-independent problem in two dimensions. For the unit cell the Hamiltonian obtained in this way is

$$\mathcal{H}(\xi,p,\tau,\mathcal{E}) = T(p) + V(\xi,\tau) + \mathcal{E}, \tag{4}$$

where $\mathcal{E}$ is canonically conjugate to τ. This ensures $\dot{\tau} = \partial\mathcal{H}/\partial\mathcal{E} = 1$. Since $\mathcal{H}$ is a conserved quantity, $-\mathcal{E}(t)$ can be interpreted as the energy ΔH that the system has gained from the driving up to time t. Moreover, it becomes clear that the dynamics is restricted to a three-dimensional "energy shell" $\mathcal{H}=\text{const}$, which is spanned by the variables ξ, p, and τ ($\mathcal{E}$ is a function of these three variables and the constant $\mathcal{H}$).

The dimensionality can be reduced further by considering Poincaré surfaces of section at some constant τ which eliminates the trivial flow in the τ direction. In the following, we shall discuss the main features of such stroboscopic surfaces of section, relevant for transport in Hamiltonian ratchets. For the moment we restrict the discussion to smooth potentials in the sense of the Kolmogorov-Arnol'd-Moser (KAM) theorem [24] and take as an example the Hamiltonian

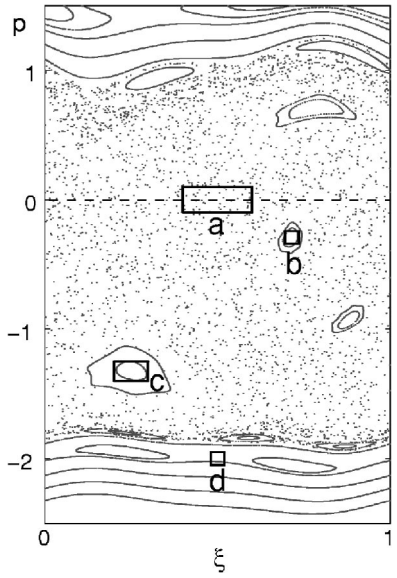

FIG. 2. Typical stroboscopic Poincaré section $\tau=0$ for a Hamiltonian ratchet with noncontractible KAM tori, main chaotic sea, and regular islands. The lettered rectangular regions support initial distributions of particles for which the corresponding velocity distributions are shown in Fig. 3 below.

$$H(p,x,t) = \frac{p^2}{2} + V_0(x) + xV_1(t) \tag{5}$$

with

$$V_0(x) = \frac{1}{5.76}[\sin(2\pi x) + 0.3\sin(4\pi x + 0.4)] \tag{6}$$

and

$$V_1(x) = -\frac{\pi}{5.76}[4.6\sin(2\pi t) + 2.76\sin(4\pi t + 0.7)]. \tag{7}$$

This corresponds to the parameter set (3) of Fig. 1 in Ref. [1] when the spatial and the temporal period are scaled to unity.

The stroboscopic Poincaré section for this model is shown in Fig. 2. We can distinguish the following three types of motion, each corresponding to a characteristic signature in phase space and transport.

(i) At high kinetic energies the ratchet potential can be considered a small perturbation acting on a free particle. For this integrable limit the trajectories are confined to invariant surfaces in phase space that have the topology of a torus. These tori are labeled by the conserved value of the momentum p and parametrized by the cyclic variables ξ and τ. In the (ξ,p) plane of the stroboscopic Poincaré section the tori would consequently appear as horizontal lines.

The KAM theorem predicts the fate of a torus under a small perturbation. It depends on whether its *winding number* w is rational or not. The winding number is the ratio

between the angular velocities along the two independent cyclic coordinates spanning the torus. In the present case, one of these coordinates is the time τ and the corresponding angular velocity is unity by definition. For the other coordinate ξ, the angular velocity on the torus is equal to the transport velocity in the extended system, measured in spatial unit cells per time period, so that $w=\bar{v}$.

Almost all tori have irrational winding numbers and, according to the KAM theorem, most of them survive an infinitesimal perturbation. This is visible in Fig. 2 at high $|p|$ where we observe lines in the stroboscopic Poincaré section which extend across the unit cell. Although the lines are deformed by the potential they represent intact tori of regular motion with irrational winding number (transport velocity). Motion proceeds on these tori in the initial direction, without turning points. As these tori cannot be continuously contracted to a point we will call them *noncontractible*.

(ii) Tori with rational winding number

$$w = \nu_x/\mu_t, \tag{8}$$

ν_x, μ_t integer, which comprise a set of measure zero, are destroyed under an infinitesimal perturbation. Details of this effect are described by the Poincaré Birkhoff theorem [24]. Together with a small neighborhood, a rational torus decays to a chaotic layer embedding new tori of regular motion. These tori have a different topology, however: They are contractible and appear as a set of μ_t regular islands in the stroboscopic Poincaré section. The respective centers of the islands are formed by a single elliptic periodic orbit with period μ_t, i.e., this orbit has μ_t distinct intersections with the stroboscopic Poincaré section before it starts repeating, shifted by ν_x unit cells in the extended space. In Fig. 2, we therefore observe chains of regular islands which are sequentially traversed by a trajectory. The average velocity of the central periodic orbit and of all trajectories inside the island corresponds to the rational winding number $\bar{v}=w$ of the destroyed torus. If $\bar{v}\neq 0$ we speak of a *transporting island*.

(iii) The chaotic regions surrounding the island chains at high $|p|$ are too small to be visible in Fig. 2. With increasing perturbation, however, the chaotic regions grow and may coalesce. In the vicinity of $p=0$ the effective perturbation is strongest. As a result a large *chaotic sea* develops. With increasing resolution we find more and more islands embedded in this sea and more and more chains of transporting islands interrupting the strips where the intact KAM tori reside. Such islands need not be remnants of rational tori in the undriven system—they can appear and disappear at some finite value of the driving potential as a result of bifurcations of periodic orbits. Still, their transport velocity must also be given by a rational winding number.

Conversely, we find more and more small chaotic regions located within the regular islands. Since they are confined to the phase-space region demarked by the outermost intact torus encircling the island, they share the same average velocity $\bar{v}=w$, where w is the winding number of the island.

The phase-space regions enumerated above are most adequately discussed in terms of *invariant sets*: a subset of the phase space invariant *as a whole* under the dynamics, irrespective of any reshuffling possibly occurring inside. For example, any regular torus in the three-dimensional phase space of the unit cell is invariant under the dynamics. Trajectories initialized on the torus do not leave it, and vice versa. This invariant two-dimensional surface separates the remaining phase space into two invariant sets of nonzero measure. Moreover, any region in phase space confined by a number of tori is an invariant set of the dynamics. In particular, this applies to the chaotic sea, which is bounded from below and above by two noncontractible KAM tori and by the outermost tori of the embedded regular islands.

For our purpose the limitation of chaotic trajectories to a compact region of phase space will be crucial. In the example discussed above this is a consequence of the KAM scenario. In systems where the KAM theorem is not valid our theory applies as long as there is another mechanism leading to a compact chaotic phase-space component. An example of this type will be discussed in Sec. II G.

C. Velocity distribution

Although the system (4) is restricted to a single unit cell, it contains the complete information about transport in the extended system (1). The velocity $v=dH/dp=T'(p)$ along a trajectory is the same in both cases provided the initial conditions are equivalent, i.e., $\xi_0=x_0 \bmod 1$ at $t=0$. Therefore the velocity is the appropriate quantity to connect transport in the extended system to the unit cell and we describe transport in terms of the velocity distribution for an ensemble of particles. An ensemble is specified by a normalized initial distribution $\rho_0(\xi_0,p_0,\tau_0)$ in the phase-space unit cell. The variable τ_0 is part of the initial conditions since it matters at which phase of the driving force a trajectory was started. It can indeed be physically meaningful to consider ensembles for which τ_0 is not sharp, for example to model a situation where particles continuously enter the system.

For any ensemble ρ_0 and time t we define the time-averaged velocity distribution as

$$P_{\rho_0,t}(v) = \frac{1}{t}\int_0^t dt' \int_{-\infty}^{+\infty} dp_0 \int_0^1 d\xi_0 \int_0^1 d\tau_0 \rho_0(\xi_0,p_0,\tau_0) \times \delta(v - T'(p_{t';\xi_0,p_0,\tau_0})) \tag{9}$$

with the normalization $\int dv\, P(v)=1$. If we consider an ensemble in the extended system, initially localized at $x=0$, then at a later time t its spatial distribution will be given in terms of the velocity distribution by $\rho_t(x)=t^{-1}P_{\rho_0,t}(x/t)$. For long times the center of mass moves with the mean velocity

$$v_{\rho 0} = \int_{-\infty}^{+\infty} dv\, v P_{\rho_0,\infty}(v), \tag{10}$$

where the existence of $P_{\rho_0,\infty}(v)=\lim_{t\to\infty}P_{\rho_0,t}(v)$ is assumed.

The behavior of the velocity distribution is qualitatively different for initial distributions ρ_0 which are restricted to different invariant sets of the phase space. This is demonstrated in Fig. 3. We used as initial distributions the characteristic functions $\chi_{a,b,c,d}$ of the rectangles marked in Fig. 2, approximated by a large number of trajectories with initial conditions distributed randomly inside the corresponding region.

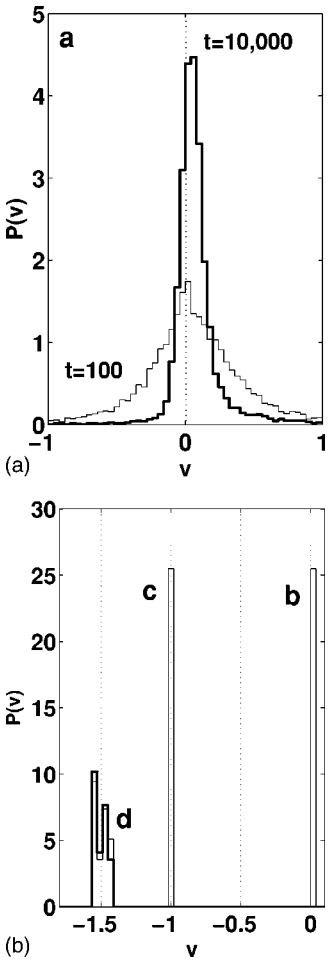

FIG. 3. Distribution of time-averaged velocities, Eq. (9), for four different initial distributions *a*–*d* (see Fig. 2). The chaotic distribution *a* was sampled by 10 000 trajectories, while for each of the regular distributions *b*–*d* only 100 trajectories were used. For each trajectory the velocity was averaged up to $t=100$ and the resulting distributions are displayed with solid lines *a*–*d*. For *a* and *d* also the distributions at $t=10\,000$ are shown (bold lines).

In the simplest case, ρ_0 has support inside a regular island (distributions *b* and *c* in Fig. 3). According to the last section, the average velocity of all trajectories inside an island is equal to the winding number *w* of the island. Consequently we have

$$P_{\rho_0,\infty}(v) = \delta(v - w) \tag{11}$$

and observe sharp peaks in Fig. 3 distributions *b* and *c* whose width is within the bin size of the histogram already at $t=100$. Figure 3 distribution *c* is an example for a transporting island, $w \neq 0$. Any distribution ρ_0 initialized inside this island will be transported ballistically with velocity $w=-1$. At the same time the width of the distribution does not grow ballistically. As stated in the Introduction, we consider this behavior as the defining property of a Hamiltonian ratchet.

For an ensemble initialized in the chaotic sea (Fig. 3 distribution *a*) the situation is similar. Although here the velocity distribution shows an appreciable width at finite times, the comparison of $t=100$ and 10 000 suggests that this width goes to zero as $t \to \infty$. We can explain this behavior using the concept of ergodicity. Ergodicity means that for any function defined on phase space and for almost all trajectories the time average along the trajectory coincides with an average over the accessible phase space. It is usually assumed that this property applies to the chaotic components of systems with a mixed phase space, although proofs of such a statement can be given only in exceptional situations [25]. For our purpose we can use the velocity $v=T'(p)$ as the function on phase space and obtain for any nonsingular initial distribution inside the chaotic sea, such as the rectangular region *a* of Fig. 2,

$$P_{\rho_0,\infty}(v) = \delta(v - v_{\mathrm{ch}}) \tag{12}$$

with the mean chaotic velocity

$$v_{\mathrm{ch}} = \mathcal{V}_{\mathrm{ch}}^{-1} \int_{\mathrm{ch}} dr\, d\xi\, d_p\, T'(p). \tag{13}$$

The phase-space integral extends here over the whole chaotic sea of the spatiotemporal unit cell, and $\mathcal{V}_{\mathrm{ch}} = \int_{\mathrm{ch}} dr\, d\xi\, dp$ denotes its volume.

In the following section we shall discuss a method to evaluate Eq. (13). For the moment it suffices to say that, in the absence of specific symmetries, there is no general reason to expect that the chaotic velocity predicted by this equation is zero. Therefore, also the chaotic sea provides an example for Hamiltonian ratchet transport.

For both regular islands and chaotic components the asymptotic velocity distribution is a δ function that does not depend on the precise location of the initial phase-space distribution within the invariant set. The velocity distribution obtained from a region with surviving noncontractible KAM tori shows a fundamentally different behavior, analogous to the case of a free particle: it maintains a finite width for $t \to \infty$ and a complicated internal structure (distribution *d* in Fig. 3). Moreover, the detailed properties of the asymptotic velocity distribution depend on the precise shape and location of the initial ensemble. Hence, according to our definition, noncontractible tori do not show ratchetlike transport.

D. Transport for invariant sets and sum rule

There is an interesting reformulation of Eq. (13) which allows us to calculate the chaotic mean velocity in terms of regular trajectories only [3]. For any subset *M* of the unit cell, we define its contribution to *transport*, $\mathcal{T}_M$, as phase-space volume times average velocity,

$$\mathcal{T}_M = \mathcal{V}_M v_M = \int d\xi\, dp\, dr\, \chi_M(\xi, p, \tau) T'(p), \tag{14}$$

where $\chi_M(\xi, p, \tau)$ is the characteristic function of *M*. Note that in this definition *M* is not necessarily an invariant set. However, if *M* denotes either the chaotic sea or a regular island, the phase-space-averaged velocity v_M can be identified with the asymptotic mean velocity of almost all trajectories inside the invariant set, as described in the previous section.

Transport has to be distinguished from the familiar con-

cept of *current* which refers to the probability flow that passes per unit time through a surface dividing phase space. Here we are interested in transport along the x direction. Therefore we consider the current at a point ξ_0. The value of the current depends on the position ξ_0 and the time τ_0 where it is measured. In terms of the density $\rho_\tau(\xi,p)$, it is given as

$$I(\xi_0,\tau_0)=\int_{-\infty}^{+\infty} dp\ \rho_{\tau_0}(\xi_0,p)T'(p). \tag{15}$$

In order to relate this current to the transport of an invariant set M, Eq. (14), we substitute the density of the invariant measure

$$\rho_\tau(\xi,p)=\frac{\chi_M(\xi,p,\tau)}{A_{M,\tau}} \tag{16}$$

where A_M denotes the area of M in a stroboscopic Poincaré section. Integration of the density over one period of the driving leads to the time-averaged current of M at ξ_0,

$$\bar{I}_M(\xi_0)=\frac{1}{A_M}\int_0^1 d\tau\int_{-\infty}^{+\infty} dp\ \chi_M(\xi_0,p,\tau)T'(p), \tag{17}$$

where we have used the conservation of phase-space area in Hamiltonian systems, $A_{M,\tau}=A_M$. An additional integration over ξ_0 yields the relation between the current in the x direction and transport

$$\mathcal{T}_M=A_M\bar{I}_M. \tag{18}$$

Here we have used that the time-averaged current is independent of the position ξ_0, as implied by the continuity equation for the invariant measure. Note that for this reason we could in principle define transport also without the ξ integration.

By choosing the density as in Eq. (16) and weighting the contribution of each invariant set M by its area A_M, we achieve that the resulting quantity, transport, is additive. Namely, with the definition (14), we have for the union of two or more disjoint sets, i.e., for $M=\cup_i M_i$, with $M_i\cap M_j=\emptyset$ for all $i\neq j$,

$$\mathcal{T}_M=\sum_i \mathcal{T}_{M_i}. \tag{19}$$

We will apply this *sum rule* for transport to the layer in phase space which contains the chaotic sea and the embedded regular islands. It is bounded from below and above by two KAM tori. For simplicity we assume that they can be represented by two functions $p_{\mathrm{u/l}}(\xi,\tau)$. We find from Eq. (14)

$$\begin{aligned}\mathcal{T}_{\mathrm{layer}}&=\int_0^1 d\xi\int_0^1 d\tau\int_{p_{\mathrm{l}}(\xi,\tau)}^{p_{\mathrm{u}}(\xi,\tau)} dp\ T'(p)\\&=\int_0^1 d\xi\int_0^1 d\tau[T(p_{\mathrm{u}}(\xi,\tau))-T(p_l(\xi,\tau))]\\&=\langle T\rangle_{\mathrm{u}}-\langle T\rangle_{\mathrm{l}},\end{aligned} \tag{20}$$

i.e., the transport of the layer is simply given by the kinetic energy T, averaged over the two bounding KAM tori. In short, since the underlying phase-space distribution $\chi_M(\xi,p,\tau)$ is flat, the transport is determined by the outline defining the subset M. This applies to *any* subset of the phase space confined by two noncontractible tori.

On the other hand, according to Eq. (19) the transport of the stochastic layer is equal to the contributions from the invariant manifolds it comprises

$$\langle T\rangle_{\mathrm{u}}-\langle T\rangle_{\mathrm{l}}=\mathcal{V}_{\mathrm{ch}}v_{\mathrm{ch}}+\sum_i \mathcal{V}_i v_i. \tag{21}$$

Equation (21) can be used to predict the chaotic transport velocity. In practice this works as follows.

(i) In the stroboscopic Poincaré section we determine the location of the limiting KAM tori $p_{\mathrm{u/l}}$ and the location of the limiting tori of all major regular islands i together with their winding numbers w_i.

(ii) In order to determine the phase-space volumes entering Eq. (21) it is in fact sufficient to know the areas in the stroboscopic Poincaré section. The Liouville theorem applied to the time-dependent Hamiltonian Eq. (1) [24] ensures that such an area is conserved by the dynamics. The three-dimensional volume within the phase space of the unit cell is simply the area at any given moment in time, multiplied by the temporal period $\mathcal{V}=A\times 1$. Areas in the Poincaré section are determined by approximating the corresponding invariant manifold by a polygon with corners obtained from running a trajectory on the outermost torus. Numerically, an approximation to this torus can be found by zooming into the Poincaré section.

(iii) The kinetic-energy averages $\langle T\rangle_{\mathrm{u,l}}$ over the bounding KAM tori are obtained by sampling a torus with a long trajectory, and determining the integrals Eq. (20) numerically. Note that this is not equivalent to a time average over such a trajectory as the invariant density on the torus is not constant.

(iv) Putting all the information together we find

$$v_{\mathrm{ch}}=\frac{\langle T\rangle_{\mathrm{u}}-\langle T\rangle_{\mathrm{l}}-\sum_i A_i w_i}{A_{\mathrm{layer}}-\sum_i A_i}. \tag{22}$$

Compared to the above procedure, the straightforward method of determining the chaotic transport velocity by running a very long trajectory has the disadvantage that its accuracy is hard to control. The trajectory must be long enough to sample the chaotic phase-space component ergodically, and there is no way to tell from a single trajectory whether this has been achieved with sufficient accuracy. The reason is that the chaotic component typically contains partial barriers (cantori), which may appear closed in a simulation over finite time. The error made by ignoring the phase-space region behind the partial barrier can in principle be arbitrarily large. Also the converse error is possible: For long simulations the accumulating numerical inaccuracy may drive a chaotic trajectory beyond an intact KAM torus. By using a stroboscopic Poincaré section such errors are substantially reduced. In the picture obtained from many relatively short trajectories, sampling the entire phase space, one can judge if there are two nearby chaotic regions which may actually form a single invariant set. It is then sufficient to increase the resolution

selectively in a small portion of the phase space, which is possible with relatively small computational effort.

E. Chaotic transport and Lévy walks

Equation (22) shows that the basic mechanism underlying chaotic ratchet transport is the existence of KAM tori and regular islands which prevent a chaotic trajectory from sampling the whole classical phase space. Unless there are special symmetries, the velocity average over the chaotic sea is generically nonzero and it is determined solely by the boundaries of this invariant set. Besides ergodicity, no reference to any details of the dynamics within the chaotic set is needed to explain and quantitatively predict the observed asymptotic chaotic transport velocity.

Nevertheless substructures inside the chaotic component of the phase space in general do exist and leave their hallmark in transport properties. Lévy walks, in particular, have attracted some attention in the context of Hamiltonian ratchets [1,4,5]. These are the episodes when a chaotic trajectory is trapped in the vicinity of a transporting island, close to the hierarchical structure of smaller and smaller islands and surrounding cantori. Such hierarchical regions are virtually unavoidable in a mixed phase space (for remarkable exceptions see [25,26]). In the context of ratchets they were termed "ballistic channels" [4,5] and are frequently located in the vicinity of the KAM tori confining the chaotic sea from below and above, i.e., in regions of relatively high velocity. Therefore Lévy walks are easily observed in numerical transport experiments. Some care must be taken to avoid the wrong conclusion that ballistic channels and Lévy walks are necessary for the existence of substantial chaotic transport or can completely account for it.

To study this question in some detail, let us start from the sum rule Eq. (19) and decompose the chaotic transport into contributions from disjunct subsets of the chaotic sea $C=\cup_j C_j$. We have $\mathcal{V}_{\rm ch}v_{\rm ch}=\Sigma_j\mathcal{V}_j v_j$ and $\mathcal{V}_{\rm ch}=\Sigma_j\mathcal{V}_{\rm j}$ such that

$$v_{\rm ch}=\frac{\sum_j \mathcal{V}_{\rm j} v_j}{\sum_j \mathcal{V}_{\rm j}}. \tag{23}$$

Because of ergodicity inside the chaotic component the phase-space volumes $\mathcal{V}_{\rm j}$ in Eq. (23) can be replaced by the fraction of time a typical chaotic trajectory spends inside subset j or, equivalently, by the probability to enter subset j times the average survival time in it. Doing so we immediately arrive at a formula similar in spirit to Eq. (3) of Ref. [4] or Eq. (6) of Ref. [5]. At the same time it is still exact and does not depend on the character of the subsets j used to subdivide the chaotic region. As in Refs. [4,5], this decomposition can, e.g., consist of a few prominent ballistic channels and some remaining chaotic "bulk" region. Our main point here is that in general it is *not* possible to approximate this remainder by an undirected and purely diffusive dynamics, i.e., to set $v_j=0$ for the corresponding subset in Eq. (23).

For this purpose we will follow the analysis suggested in Refs. [4,5] but apply it to a model with different parameter values. The Hamiltonian is

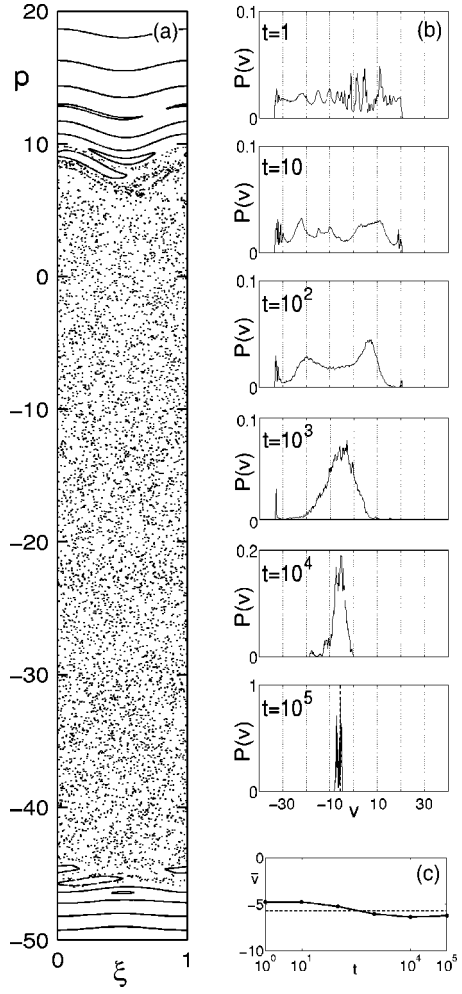

FIG. 4. (a) Stroboscopic Poincaré section at $\tau=0$ for the system of Eq. (24). (b) For an initial distribution $\rho_0\sim\chi_{\rm ch}$ the distribution of time-averaged velocities is shown at various times t. As $t\to\infty$ it evolves to a narrow peak around the asymptotic mean velocity (dashed line for $t=10^5$). (c) From all distributions shown in (b) the average velocity $\bar{v}$ is computed after the contributions from the ballistic channels have been removed by restricting $P(v)$ to the interval $-28\leqslant v\leqslant +18$. The resulting values (dots) are for all times close to the asymptotic mean velocity (dashed).

$$H(p,x,t)=\frac{p^2}{2}-2\pi\cos(2\pi x)+(2\pi)^2 x\left[2\cos(2\pi t)-4\cos\left(4\pi t+\frac{\pi}{2}\right)\right] \tag{24}$$

and the stroboscopic Poincaré section [Fig. 4(a)] shows the typical features discussed in Sec. II B. The velocity distribution of the chaotic component is shown in Fig. 4(b) for various times. In contrast to Fig. 3 distribution c we have chosen here an ensemble of initial conditions $\rho_0\sim\chi_{\rm ch}$ uniformly covering the entire chaotic sea. Numerically this has been achieved by relying on ergodicity. We ran a single long chaotic trajectory $x(t)$ $(0\leqslant t\leqslant 4\times10^5)$ and used $x(t')$ with $t'=0,1,2,\ldots$ as the initial conditions of the ensemble. For

each such initial condition $\bar{v}_t=[x(t'+t)-x(t')]/t$ is the velocity averaged over a time span t. For fixed t the probability distribution $P(\bar{v}_t)$ is shown in Fig. 4(b). It is equivalent to the propagator used in Ref. [5] for visualizing internal details of the chaotic dynamics. Peaks in the propagator can be interpreted as signatures of partial transport barriers within the chaotic sea. They are visible as long as the parameter t of the velocity distribution is smaller than the time scale for crossing the barrier. As expected, for long times ($t>10^5$) only a narrow peak survives at a velocity which is in good agreement with the prediction of the sum rule (dashed line for $t=10^5$).

Since the shape of the velocity distribution depends strongly on time, any definition of ballistic channels and the corresponding subdivision of the chaotic invariant set must be highly arbitrary. We single out the most prominent transporting islands which are visible in Fig. 4(a) close to the lower and the upper boundaries of the chaotic sea. They have winding numbers $w_-\sim 30$ and $w_+\sim 20$, respectively. In these regions we observe particularly sharp peaks in the velocity distribution for $t\lesssim 10^3$ which are signatures of the corresponding Lévy walks. Following Ref. [5] we continue by averaging the velocity distribution over a region that excludes all such ballistic channels [$-28\leqslant v\leqslant +18$ for the solid line in Fig. 4(c); note that this v interval is defined with respect to the average velocity and therefore is not completely inside the chaotic layer in the Poincaré section shown in Fig. 4(a)]. The result represents the contribution from the bulk of the chaotic sea. It is definitely nonzero and in fact quite close to the asymptotic transport velocity (dashed line), irrespective of the time scale and the precise cutoff values used. In other words, the average chaotic transport in this example is mainly due to the bulk region while the ballistic channels and their Lévy walks contribute small corrections only.

This shows that only the invariant sets, as featured in the sum rule Eq. (19), provide an appropriate concept for the description of the asymptotic directed transport.

F. Biased ratchets

Can Hamiltonian ratchets be used to transport particles against an external force? As explained in Sec. II A, a constant force does not destroy the periodicity of the dynamics, and we can still resort to a unit cell to understand the transport properties. The key question is, which invariant sets may survive in presence of an additional potential $V_{\text{bias}}(x)=cx$. In Fig. 5(a) we compare two trajectories for $c=0.13$ to the familiar phase-space portrait at $c=0$ (Fig. 2). One of them was initialized on a large transporting island with winding number $w=1$. Clearly, this island is still present although it is distorted and shifted in position. The winding number of the island is conserved since it is a topological quantity restricted to rationales. Hence all trajectories inside the islands have asymptotic mean velocity $\bar{v}=1$ and we may conclude that Hamiltonian ratchets can transport uphill. This is confirmed by the full line in Fig. 5(b), which shows position vs time for the same trajectory.

The other trajectory was initialized in a phase-space region which for $c=0$ contains noncontractible KAM tori with

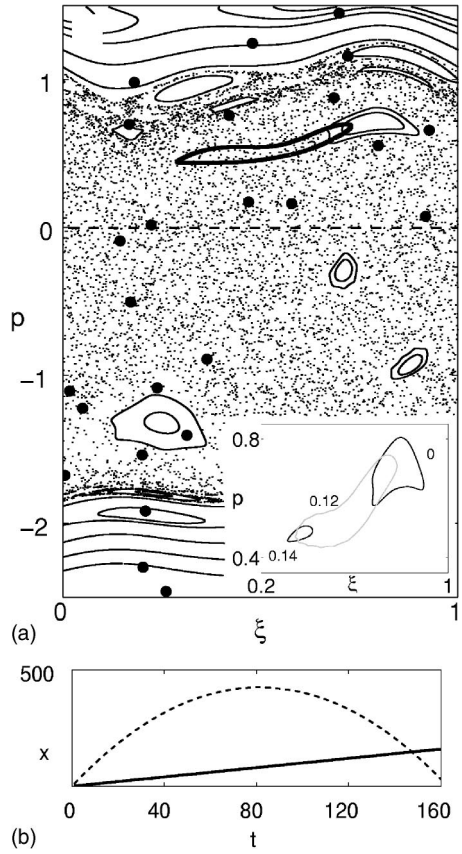

FIG. 5. (a) Stroboscopic Poincaré section for the model Eq. (5) as in Fig. 2. On top two trajectories of a system with the additional potential $V_{\text{bias}}(x)=cx$ with $c=0.13$ are shown. One trajectory (big dots) was started at $p=10$, i.e., in a phase-space region which is in the original system filled by noncontractible regular tori. In the presence of the bias such tori are absent and the trajectory keeps losing momentum without bounds. In the extended system this trajectory is similar to a parabola [dashed line in (b)]. The other trajectory [thick line in (a) and (b)] is part of a regular island with winding number $w=1$, i.e., in the extended system this trajectory is transporting uphill without losing momentum. The inset of (a) shows the shape of the regular island at different magnitudes of the bias potential. At $c\gtrsim 0.15$ the island disappears. Also islands with negative or zero winding number do exist in the biased ratchet (not shown).

positive winding numbers. We observe that for $c=0.13$ the momentum of this trajectory is decreasing without bounds under the influence of the constant bias force, as naive expectation suggests. Only in a short time interval, when $p_t\approx 0$, the driving potential has a relevant influence on this trajectory. For long times it behaves essentially like a free particle accelerated by the bias potential. Therefore $x(t)$ for this trajectory is approximately parabolic [dashed line in Fig. 5(b)].

From the presence of this single accelerated trajectory we can already conclude that no regular KAM tori survive in the biased system (at least not in the phase-space region displayed in Fig. 5), since these would represent impenetrable barriers to transport in the p direction. Note that the KAM theorem does not apply to this situation: A constant force does not represent a smooth perturbation for the unit cell

since the potential is not periodic. In fact there is a simple argument suggesting that an arbitrary small mean force destroys all noncontractible KAM tori. Assume that there is a KAM torus of the form $p(\xi,\tau)$ periodic in ξ and τ. Consider its average momentum at some given moment in time,

$$\bar{p}(\tau) = \int_0^1 d\xi\, p(\xi,\tau). \tag{25}$$

As we show by a straightforward calculation in Appendix A the increment of $\bar{p}$ after one temporal period is given by

$$\bar{p}(\tau+1) - \bar{p}(\tau) = -\int_0^1 d\xi\, d\tau\, V'(\xi,\tau). \tag{26}$$

Clearly, this increment must vanish for an invariant KAM torus. However, the right-hand side (RHS) of Eq. (26) is not zero for a biased system with a mean force. We conclude that no extended KAM tori survive and that therefore the chaotic sea is no compact invariant set anymore. Hence an arbitrarily small bias potential will destroy the chaotic ratchet transport in models like Eq. (5) while uphill transport can be realized by preparing initial conditions on regular islands of the phase space.

G. A minimal model

According to the previous sections, the decisive property of a Hamiltonian ratchet is an asymmetric mixed phase space. Based on this insight we can now construct minimal models for Hamiltonian ratchets which have this property and are otherwise as simple as possible. Probably the simplest type of model with a mixed phase space are area-preserving maps generated from kicked one-dimensional Hamiltonians of the form

$$H(x,p,t) = T(p) + V(x)\sum_n \delta(t-n). \tag{27}$$

Integrating the equations of motion over one period of the driving we obtain an explicit map expressing position x_n and momentum p_n immediately before the kick at $t=n$ in terms of the values before the preceding kick

$$p_{n+1} = p_n - V'(x_n), \quad x_{n+1} = x_n + T'(p_{n+1}). \tag{28}$$

The most prominent example is the kicked rotor

$$T(p) = \frac{p^2}{2}, \quad V(x) = \frac{K}{2\pi}\cos(2\pi x), \tag{29}$$

one of the best-studied paradigms of Hamiltonian chaos [27]. The phase space of this model is periodic with period 1 both in x and in p. Therefore one can define a compact unit cell with area $\Delta x\,\Delta p = 1$.

The kicked rotor found an important experimental realization in the dynamics of cold atoms in pulsed laser fields [28,29]. In this experimental setup the momentum instead of the position is the experimentally accessible quantity and one is therefore interested in transport along the momentum direction. Apart from this purely formal difference, atom optics experiments promise to be ideal realizations of Hamiltonian ratchets. For this purpose one has to modify the phase space of the unit cell such that transporting islands arise and the symmetry $x \to -x$, $p \to -p$ of the kicked rotor is destroyed.

In fact transporting islands appear already in the standard kicked rotor at kicking strengths $K \gtrsim 2\pi m$. They are referred to as "accelerator modes" [27] and leave traces in the dynamics which were also experimentally observed [29]. In the kicked rotor these accelerator modes always come in pairs transporting in opposite directions and therefore do not lead to transport in the chaotic sea. However, this symmetry can be destroyed, e.g., by applying more than a single kick per period or by using asymmetric potentials in Eq. (27). It is not expected that the details of these manipulations will be of importance for the resulting chaotic transport since, as we have shown in the previous sections, the latter is determined by the underlying phase-space structure only.

In the remainder of this paper we therefore study an abstract model in the form of Eq. (28). The functions $T(p)$ and $V(x)$ are selected without reference to any particular experimental setup and only guided by the desire to have a simple phase-space structure with a large transporting island. We choose

$$V(x) = (x \bmod 1 - 1/2)^2/2,$$

$$T(p) = |p| + 3\sin(2\pi p)/(4\pi^2). \tag{30}$$

The resulting map

$$p_{n+1} = p_n - (x_n \bmod 1) + 1/2,$$

$$x_{n+1} = x_n + \mathrm{sgn}(p_{n+1}) + 3\cos(2\pi p_{n+1})/2\pi \tag{31}$$

is considered on a cylinder with transport along the extended x axis while $p \equiv p+1$ is here a cyclic variable that can be represented by $p \in [-1/2, +1/2)$. If the map is restricted to one unit cell $x \to \xi = x \bmod 1$ we obtain the phase-space portrait shown in Fig. 6(a). It shows one large regular island around the stable fixed point $\xi_0 = 1/2$, $p_0 = -1/4$ with winding number $w_0 = -1$. Due to the term $|p|$ in $T(p)$ the phase space has no reflection symmetry around $p=0$ and also no other momentum-inverting symmetry such that there is no equivalent island transporting in the positive direction.

There are also no extended regular tori and the whole unit cell must be considered as the analog of the compact stochastic layer in the continuously driven models which we considered in the previous sections. Consequently the LHS of the sum rule Eq. (21) vanishes, $0 = v_{\mathrm{ch}}\mathcal{V}_{\mathrm{ch}} + (-1)\mathcal{V}_{\mathrm{reg}}$. In other words the total transport, averaged over the whole available phase space, vanishes for this system which confirms that it is unbiased. A considerable simplification results from the fact that here the chaotic transport velocity can be computed from the relative phase-space volume of the single regular island $A_{\mathrm{reg}} = 1 - A_{\mathrm{ch}}$ alone,

$$v_{\mathrm{ch}} = A_{\mathrm{reg}}/(1 - A_{\mathrm{reg}}). \tag{32}$$

From the Poincaré section Fig. 6(a) we find $A_{\mathrm{reg}} = 0.117 \pm 0.001$; thus $v_{\mathrm{ch}} = 0.133 \pm 0.001$. This is in very good agreement with $v_{\mathrm{ch}} = 0.1344 \pm 0.0003$ obtained directly from the spatial distribution of 10^4 trajectories after 2×10^4 kicks.

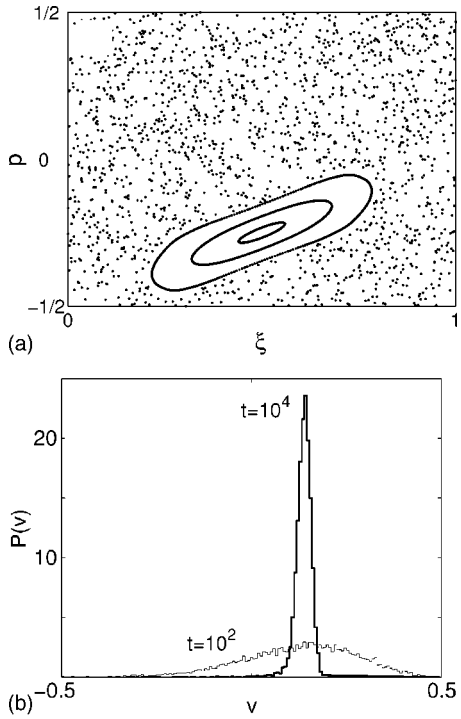

FIG. 6. (a) Poincaré section p vs ξ of a unit cell for the map given by Eq. (31). (b) Velocity distribution $P(v)$ of 10^4 trajectories started at random on the line $p=0$, $x\in[0,1)$ in the chaotic sea of the system and iterated until 10^2 and 10^4, respectively.

Figure 6(b) shows the convergence of the chaotic velocity distribution to a δ function concentrated at this value, in accordance with Eq. (11).

We would like to stress again that the directed chaotic transport in this ratchet model is a consequence of the phase-space structure and cannot be explained by the asymmetric kinetic-energy function alone. We have verified this fact by repeating the analysis for a larger potential $5V(x)$. Then the phase space is completely chaotic, yet despite the asymmetric function $T(p)$ no transport is observed.

III. QUANTUM RATCHETS

We now turn to the investigation of quantized Hamiltonian ratchets, i.e., driven one-dimensional Hamiltonian quantum systems which are classically periodic both in space and in time. We restrict attention to systems in which the phase-space volume of a unit cell is finite and phase space is composed of a chaotic sea with one or more embedded regular islands, as in the minimal ratchet model discussed above. This restriction leads to a finite Hilbert-space dimension which simplifies the numerical calculations. Moreover, we have seen that the dynamical processes relevant for transport are restricted anyway to the compact chaotic layer of the unit cell. We therefore expect models with finite Hilbert-space dimension to capture also the essential features of quantized ratchet transport.

A. Floquet operator and eigenstates

For a system periodic in time, one can still construct a dynamical group with a single timelike parameter, which, however, now becomes discrete, measuring time in units of the period of the driving. It is generated by the unitary evolution operator over one period,

$$\hat{U}(t+1,t)=\hat{\mathcal{T}}\exp\left(-\frac{i}{\hbar}\int_0^1 dt\,\hat{H}(t)\right), \tag{33}$$

where $\hat{\mathcal{T}}$ effects time ordering. The computation of this Floquet operator is simplified considerably if $H(t)$ is a kicked Hamiltonian as in Eq. (27). Then the time evolution from time $t=m-\varepsilon$ immediately before the kick m to time $t=m+1-\varepsilon$ immediately before the following kick can be expressed in terms of $T(p)$ and $V(x)$ as a product

$$\hat{U}=e^{-iT(\hat{p})/\hbar}e^{-iV(\hat{x})/\hbar} \tag{34}$$

of two operators which are diagonal in the position or the momentum representation, respectively. The time evolution of a state is obtained by successive multiplications by phase factors and fast Fourier transforms effecting a basis change. An additional simplification results if we consider p as a cyclic variable $p\equiv p+1$, as is the case with the minimal ratchet model Eq. (31) to which our numerical results will be restricted. In this case the wave function is periodic in p with $\psi(p+1)=\psi(p)$ and consequently the conjugate variable x is restricted to the discrete values $x_n=nh$. Here, h denotes the dimensionless ratio of Planck's constant to the phase-space area of the classical unit cell which we set to unity in Eq. (31). It is a well-known peculiarity of models with this property that the periodicity of the classical potential $V(x+1)=V(x)$ [or at least $V'(x+1)=V'(x)$ in the case of our minimal model] does not necessarily lead to a spatially periodic Floquet operator. The reason is that the potential is now restricted to discrete values $V_n=V(x_n)=V(nh)$ and periodicity is achieved only if there is an integer N with $V_{n+N}=V_n$ which implies $hN=M$ with another integer M. Hence $h=M/N$ must be rational. In contrast, in periodic systems with infinite phase-space volume such as Eq. (5), the Floquet operator is spatially periodic irrespective of the value of Planck's constant. In the following sections we shall use values $h=1/N$ to ensure that the quantum system has the same spatial periodicity as the classical model. Only in the last Sec. III D do we consider modifications of our results for irrational values of h. They are to be interpreted as a spatial disorder that does not affect the classical phase-space structure but destroys the perfect periodicity of the corresponding quantum system.

A double periodicity, in both space and time, requires to combine the corresponding representations of quantum mechanics appropriate for these symmetries, i.e., Bloch and Floquet theory, respectively. The eigenvalue equation

$$|\phi_\alpha(t+1)\rangle=\hat{U}|\phi_\alpha(t)\rangle=e^{-2\pi i\epsilon_\alpha}|\phi_\alpha(t)\rangle \tag{35}$$

defines *Floquet states* $|\phi_\alpha\rangle$ and *quasienergies* $\epsilon_\alpha\in[0,1)$ [30]. For the systems considered here α is a discrete index $1\leqslant\alpha\leqslant N$.

For the discrete spatial translation group there is a continuous set of representations parametrized by the quasimomentum $k\in[0,1)$. In the simultaneous presence of temporal periodicity, the Bloch theorem now applies to Floquet states,

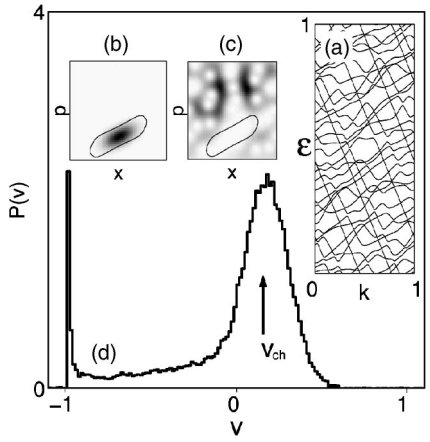

FIG. 7. (a) Quasienergy band spectrum of the minimal ratchet model Eq. (31) at $h^{-1}=32$. Regular bands appear as approximately straight lines with negative slope. (b) The Husimi representation of the Floquet eigenstates corresponding to points on these lines are concentrated inside the regular island. (c) Most other eigenfunctions spread over the entire chaotic sea but avoid the regular island. The corresponding bands have strongly fluctuating slopes. (d) Distribution of band slopes (velocity expectation values) at $h^{-1}=128$. The sharp peak at $v=-1$ corresponds to the regular bands, the broader peak to the chaotic bands. The velocity of the classically chaotic transport is marked by an arrow.

$$\phi_{\alpha,k}(x+1,t) = e^{2\pi ik}\phi_{\alpha,k}(x,t) \tag{36}$$

so that both eigenstates and eigenphases carry a double index (α,k). The support of the *Floquet band spectrum*, in all cases considered here, consists of continuous lines in the two-dimensional (k,ϵ) space; cf. Fig. 7(a). Since the spectrum is periodic with period 1 in both ϵ and k, these variables are canonically conjugate to a pair of integers (n_x,m_t) which measure position and time in units of the spatial and temporal periods, respectively. For this reason the band structure and the time evolution of the spatial distribution are related by a double Fourier transformation, as we shall show in Sec. III B.

We have seen that the decisive property of classical Hamiltonian ratchets is the existence of invariant sets of the phase space with different average velocities. Traces of the classically invariant sets are manifest in the quantum dynamics only if the quantum uncertainty allows their resolution, i.e., if $\hbar$ is much smaller than the relevant phase-space structures. From here on we shall restrict our attention to this semiclassical regime. Figure 7(a) shows an example of a Floquet band spectrum for a Hamiltonian ratchet, the minimal model (31). This system has two distinct invariant sets in phase space, the chaotic sea and one transporting island embedded in it. According to the semiclassical eigenfunction hypothesis [31,32] one expects that in the semiclassical regime almost all eigenfunctions condense on one of the invariant phase-space sets. Figures 7(b) and 7(c) show the Husimi representations [33] of typical eigenstates. Indeed, one of them is concentrated inside the regular island while the other populates the chaotic sea, avoiding the island. Associated with these two types of eigenstates are two types of bands: regular bands appear in the spectrum as straight lines with slope $d\epsilon_\alpha/dk \approx -1$, chaotic bands are fluctuating and have on average a positive slope. In the subsequent section, we are going to make this relation between bands and subsets of the phase space more precise. We use it to establish a sum rule for transport in quantum ratchets analogous to the classical sum rule discussed in Sec. II D.

B. Semiclassical transport in terms of Floquet bands

1. Quantum sum rule

The basic relation expressing the velocity of a Floquet state in terms of the quasienergy band to which it belongs is

$$v_{\alpha,k} = \langle\langle \phi_{\alpha,k}|\hat{v}|\phi_{\alpha,k}\rangle\rangle = \frac{d\epsilon_{\alpha,k}}{dk}. \tag{37}$$

In the present case of a periodically driven system, the expectation value of the velocity operator $\hat{v}=\hat{T}'(\hat{p})$ includes a time average over one period of the driving $\langle\langle\cdots\rangle\rangle \equiv \int_0^1 dt\langle\cdots\rangle$. The second member of Eq. (37) then follows from applying the Hellmann-Feynman theorem, which was proven for time-periodic systems in [30].

A wave packet localized on the scale of a single unit cell or narrower corresponds to a nearly homogeneous distribution in k. The corresponding mean velocity for a whole band α vanishes,

$$\langle v_\alpha\rangle_k = \int_0^1 dk \frac{d\epsilon_{\alpha,k}}{dk} = 0, \tag{38}$$

as is implied by the periodicity of the bands. Averaging also over energy, i.e., summing over the bands, we find as velocity average over the total Hilbert space of the unit cell,

$$\langle v\rangle_{k,\epsilon} = \frac{1}{N}\sum_\alpha \left\langle \frac{d\epsilon_{\alpha,k}}{dk}\right\rangle_k = 0. \tag{39}$$

Equation (39) can be considered the quantum-mechanical counterpart of the classical sum rule for transport, Eq. (21). Effectively, the quantum sum rule like the classical one refers to a finite subset of the phase space. Here, the cutoff is introduced by the finite dimension of the basis used to span the Hilbert space of the unit cell in calculating the band spectrum.

The crucial step for this quantum sum rule is the averaging along a given band α over the entire Brillouin zone, Eq. (38). In particular, this amounts to regarding all band crossings, however narrow, as avoided crossings. If k were considered a parameter with a fictitious time dependence, the quantum time evolution under a slow change of k would respect avoided crossings in exactly this manner. Therefore these bands are referred to as *adiabatic bands* [34].

It follows, conversely, that a finite mean velocity can be obtained if modified bands are constructed by connecting band segments *across* all avoided crossings with a gap below some threshold. Such bands determine the time evolution under a fast change of k and accordingly are called *diabatic* [34]. They are not associated with a fixed band index α and therefore need not be periodic in k. So for individual diabatic

bands Eq. (38) does not apply, their mean velocity can be finite. We argue in the following that indeed it is diabatic bands, not adiabatic ones, which semiclassically correspond to invariant sets of classical phase space, and to which a relation between band structure and directed transport must refer.

Figure 7 provides numerical evidence to justify the assignment of invariant sets to diabatic bands. For example, the regular island with winding number -1 is associated with straight-line segments in the spectrum, corresponding to a quantum velocity $v_{\alpha,k}=-1$ with very small fluctuations. In contrast, chaotic regions are represented by "wavy" band sections with strongly varying slope to which a precise velocity value cannot be assigned. In this sense, it is legitimate to talk of "regular" vs "chaotic" diabatic bands.

In the following we will reconsider the sum rule Eq. (39) using diabatic bands and express the different contributions in terms of the invariant sets of the classical phase space. First we note that replacing in Eq. (39) adiabatic by diabatic bands amounts to interchanging band indices at avoided crossings, thus it results at most in a permutation of terms within the sum but does not affect the sum rule as a whole. We can therefore group diabatic-band terms in Eq. (39) according to the classical invariant set they pertain to,

$$0 = \sum_{\alpha\in\text{ch. bands}} \left\langle \frac{d\epsilon_{\alpha,k}}{dk} \right\rangle_k + \sum_{r\in\text{reg. bands}} \left\langle \frac{d\epsilon_{r,k}}{dk} \right\rangle_k . \quad (40)$$

In the semiclassical limit the respective numbers of terms in the sums are given by the relative fraction of the phase space occupied by the corresponding invariant sets, i.e., $N_{\text{ch}}=f_{\text{ch}}N$ for the chaotic bands and $N_r=f_rN$ for the various embedded regular islands r. $N=h^{-1}$ is here the total number of bands, i.e., the Hilbert-space dimension per unit cell. Assuming that the classical phase space contains only a single chaotic component we can characterize the associated diabatic bands by a mean slope $\langle v_{\text{ch}}\rangle$ and have $\Sigma_{\alpha\in\text{ch}}\langle d\epsilon_{\alpha,k}/dk\rangle_k=N_{\text{ch}}\langle v_{\text{ch}}\rangle$.

For the regular bands, the double periodicity of the (k,ϵ) space allows us to define *winding numbers* in the same way as we did in Sec. II B for the topology of regular islands in the conjugate (x,t) space. For the same reason as with the classical winding numbers these topological quantum numbers have to be rational, i.e., $w^{\text{qm}}=n/m$ if the band closes upon itself after n revolutions in the ϵ and m revolutions in the k direction. As the regular states are localized on the invariant tori inside the island, their velocity expectation (band slope) in the semiclassical limit approaches the regular transport velocity. This leads to the conclusion

$$\left\langle \frac{d\epsilon_r}{dk} \right\rangle_k \approx w_r^{\text{qm}} = w_r^{\text{cl}} = v_r^{\text{cl}} . \quad (41)$$

Avoided crossings modify the band slopes in a range which is negligible in the semiclassical limit (see Sec. III C), while the winding numbers as topological quantities are not affected at all. In other words, the winding number w_r^{qm} of a diabatic band r pertaining to a classical regular island r is *identical* to the classical winding number w_r^{cl} of that island, Eq. (8). We have now

$$0 = Nf_{\text{ch}}\langle v_{\text{ch}}\rangle + N\sum_r f_r v_r^{\text{cl}} . \quad (42)$$

Note that f_{ch}, f_r, and v_r^{cl} are all *classical* quantities. Consequently, also the quantum transport velocity $\langle v_{\text{ch}}\rangle$ must coincide with its classical counterpart

$$\langle v_{\text{ch}}\rangle = v_{\text{ch}}^{\text{cl}} . \quad (43)$$

This is the main result of the quantum-mechanical sum rule. We stress again that it pertains to the semiclassical regime since otherwise the notion of diabatic bands is not applicable.

Figure 7(d) confirms Eq. (43) qualitatively. It shows the distribution of quantum velocities (band slopes) for our minimal ratchet model. We observe two well-separated peaks, one for the regular bands at $v_r^{\text{cl}}=-1$ and one at $v_{\text{ch}}^{\text{cl}}$ for the chaotic bands. The region separating the two peaks corresponds to the band slopes in the vicinity of avoided crossings between regular and chaotic bands. The weight of the distribution in this intermediate region decreases with h and vanishes in the semiclassical limit $h\to 0$.

2. Form factor

Our analysis based on winding numbers can be applied to predict the mean quantum transport velocity in the semiclassical regime from the classical value. The band spectra, however, contain more detailed information about quantum transport, encoded in the spectral two-point correlation functions. A double Fourier transform $\epsilon\to m_t$, $k\to n_x$ and subsequent squaring of the spectral density translates two-point correlations in the bands into the entire time evolution of the spatial distribution on the scale of the temporal and spatial periods, respectively.

As a suitable quantity to establish this relation, we recur to the generalized form factor introduced and studied in [35] for completely chaotic systems. We define it as

$$K(n_x,m_t) = \frac{1}{N}\langle |u(n_x,m_t)|^2\rangle \quad (44)$$

with

$$\begin{aligned} u(n_x,m_t) &= \int_0^1 dk\, e^{2\pi i k n_x} \text{tr} U_k^{m_t} \\ &= \sum_{\alpha=1}^{N} \int_0^1 dk\, e^{2\pi i (k n_x - \epsilon_{\alpha,k} m_t)} \\ &= \sum_{\alpha=1}^{N} u_\alpha(n_x,m_t) . \end{aligned} \quad (45)$$

N denotes the Hilbert-space dimension per unit cell, which is the phase-space area of a unit cell in units of Planck's constant h. U_k is the $N\times N$ Floquet operator (33) evaluated at Bloch number k. The integers n_x,m_t are the discrete variables canonically conjugate to k and ϵ, respectively, that is, the unit cell number relative to the starting point, and time in units of the period of the driving. The average $\langle\cdots\rangle$ in Eq. (44) is essential in order to remove the otherwise dominant

fluctuations around the mean value. It can be taken over a narrow time range or over an ensemble of quantum systems corresponding to approximately the same classical system.

As we will now show, the form factor is related, on the one hand, to the classical dynamics of a distribution which initially covers homogeneously the phase space of a single unit cell. On the other hand, it contains the quantum velocity distribution as a limiting case. Therefore it is an appropriate starting point for a semiclassical theory of ratchet transport.

We assume we are sufficiently close to the semiclassical limit $N \gg 1$ such that we can consider the band spectrum in the diabatic approximation. Moreover, in the semiclassical limit it is justified to neglect correlations between diabatic bands pertaining to different invariant sets (regular or chaotic) unless they are related by symmetries. This allows us to write the form factor as an incoherent sum of the respective contributions, because the averaging in Eq. (44) suppresses uncorrelated cross terms. We obtain

$$K(n_x,m_t) = \sum_r K_r(n_x,m_t) + K_{\mathrm{ch}}(n_x,m_t), \tag{46}$$

the sum running over all regular invariant sets (islands and island chains).

In Appendix B we obtain the semiclassical expression

$$K_r(n_x,m_t) = f_r \mu_r \delta_{\mu_r n_x - \nu_r m_t} \tag{47}$$

for the form factor of a chain of regular islands with winding number $w_r = \nu_r/\mu_r$. It seems that the form factor is enhanced by a factor μ_r for an island chain as compared to a single island of equal total size, but this is not the case. In Eq. (47), $\delta_{\mu_r n_x - \nu_r m_t} = 1$ holds only at the unit cell $n_x = (\nu_r/\mu_r) m_t = v_r m_t$ to which a classical trajectory, started in the regular island at $n_x = 0$, has traveled in time m_t. In particular, as n_x is an integer, m_t must be an integer multiple of μ_r. That is, $K_r(n_x,m_t)$ is finite only every μ_rth period of the driving, such that the average contribution to the form factor is independent of the period μ_r of the island chain.

For the chaotic contribution to the form factor we can resort to a semiclassical theory which has been developed for completely chaotic systems in [35,36]. In order to apply it to a system with a mixed classical phase space we assume the validity of the ergodic sum rule [37] for the chaotic component. Then the result of [35,36] remains essentially unchanged, and the form factor is given in terms of the classical velocity distribution of the chaotic component as

$$K_{\mathrm{ch}}(n_x,m_t) = \frac{m_t}{m_{\mathrm{H}}} P_{\mathrm{ch}}\left(\frac{n_x}{m_t}, m_t\right) \quad (m_t \lesssim m_{\mathrm{H}}). \tag{48}$$

To be precise, $P_{\mathrm{ch}}(v,t)$ entering this equation is the chaotic classical propagator for a uniform distribution inside the chaotic sea, as introduced in Sec. II E. Its definition is Eq. (9) with $\rho_0 = \chi_{\mathrm{ch}}$. Since Eq. (48) is based on the diagonal approximation [38], i.e., correlations between different classical orbits have been neglected, it is valid only for short times and breaks down beyond the Heisenberg time $m_{\mathrm{H}} \approx N_{\mathrm{ch}} \approx f_{\mathrm{ch}} N$ of the chaotic component.

3. Quantum velocity distribution

A complementary approximation to the form factor for long times can be achieved following again Refs. [35,36]. The chaotic bands fluctuate as a function of k with an amplitude approximately given by the spacing $\Delta\epsilon \approx N_{\mathrm{ch}}^{-1}$ between them. For times beyond the Heisenberg time, these fluctuations give rise to phase oscillations in the integrand of Eq. (45) which exceed 2π. Therefore we can perform the k integration in stationary-phase approximation and obtain

$$u_\alpha(n_x,m_t) = \sum_{\epsilon'_{\alpha,k_s} = n_x/m_t} \sqrt{i/|\epsilon''_{\alpha,k_s} m_t|} \exp(2\pi i [k_s n_x - \epsilon_{\alpha,k_s} m_t]), \tag{49}$$

i.e., only those points $k = k_s$ contribute to the integral where the derivative of the phase of the integrand vanishes, $0 = n_x - \epsilon'_{\alpha,k_s} m_t$. These are isolated points in the spectrum which can be assumed to vary independently upon averaging in Eq. (44). Therefore we can neglect all cross terms when squaring the sum of contributions from different points of stationary phase and obtain for the form factor

$$K_{\mathrm{ch}}(n_x,m_t) = \frac{1}{m_{\mathrm{H}} m_t} \sum_\alpha \sum_{\epsilon'_{\alpha,k_s} = n_x/m_t} |\epsilon''_{\alpha,k_s}|^{-1}. \tag{50}$$

Now that we are rid of all phase factors it is very instructive to rewrite the result again as an integral over the Bloch number k,

$$K_{\mathrm{ch}}(n_x,m_t) = \frac{1}{m_{\mathrm{H}} m_t} \sum_\alpha \int_0^1 dk\, \delta\left(\epsilon'_{\alpha,k} - \frac{n_x}{m_t}\right). \tag{51}$$

This equation has two important consequences. First we note that up to normalization the form factor beyond the Heisenberg time is nothing but the distribution of band slopes, alias quantum velocities,

$$K(n_x,m_t) \sim P_{\mathrm{quant}}(v)|_{v = n_x/m_t} (m_t > m_{\mathrm{H}}), \tag{52}$$

which is shown for the minimal model in Fig. 7(a). As in the classical case, this velocity distribution is the natural quantity to describe a system with directed ballistic quantum transport and the form factor can be considered a useful generalization of it.

Second, Eq. (51) implies that the form factor at any time m_t beyond the Heisenberg time m_{H} can be expressed via scaling by the form factor right at the Heisenberg time

$$K_{\mathrm{ch}}(n_x,m_t) = \frac{m_{\mathrm{H}}}{m_t} K_{\mathrm{ch}}\left(m_{\mathrm{H}} \frac{n_x}{m_t}, m_{\mathrm{H}}\right) = \frac{m_{\mathrm{H}}}{m_t} P_{\mathrm{ch}}\left(\frac{n_x}{m_t}, m_{\mathrm{H}}\right) \quad (m_t > m_{\mathrm{H}}). \tag{53}$$

In the second line we have used the semiclassical approximation Eq. (48) for $m_t = m_{\mathrm{H}}$. It is valid only up to the Heisenberg time, but according to Eq. (51) it determines the form factor also beyond. Of course, the validity of Eq. (53) depends on applying both the short-time and the long-time approximations for the form factor right at the Heisenberg time where they are on the verge of breaking down. This interpo-

lation procedure has been corroborated by comparison to results from numerics and from supersymmetry in [35,36]. We expect that it applies in the present case of a transporting chaotic component as well.

The two consequences of Eq. (51) combine to the conclusion that the distribution of quantum velocities in the chaotic component of the band spectrum is equal to the distribution of time-averaged classical velocities for an ensemble of particles filling the chaotic component of the phase space homogeneously. Information on the quantum system enters into this classical distribution only via the point in time at which this velocity distribution is evaluated—it must be chosen as the Heisenberg time N_{ch} of the chaotic component. Before writing down this result we note that the restriction to the chaotic component is actually not necessary, since for the embedded regular islands the same result applies trivially because of Eq. (41). Hence we have

$$P_{\mathrm{quant}}(v) = P_{\mathrm{class}}(v, m_{\mathrm{H}}), \tag{54}$$

for a stochastic layer including one chaotic component and one or more embedded regular islands. Equation (54) is a nontrivial result because it establishes quantum-classical correspondence for the velocity distributions and thus for asymptotic *long-time* transport properties. We stress again that this result was derived semiclassically within the diagonal approximation. It would be very interesting to explore possible corrections due to neglected interferences between classical periodic orbits (akin to the weak-localization correction in the standard form factor [38]), but at present the methods to deal with such corrections [39] are not sufficiently developed to treat the type of system we are dealing with here.

C. Long-time quantum transport and dynamical tunneling

1. Transport of wave packets

So far we have considered transport only in terms of stationary quantities like eigenstates and band spectrum. Using the obtained results we can now describe the transport of arbitrary wave packets. The asymptotic quantum transport velocity of a wave packet is an average over all band slopes, weighting each Floquet state by its overlap with the initial state. To see this we write the wave packet as a superposition of Floquet states

$$\begin{aligned}\psi(x,t) &= \sum_{\alpha} \int_0^1 dk\, \psi_{\alpha,k}(t)\, \phi_{\alpha,k}(x) \\ &= \sum_{\alpha} \int_0^1 dk\, \psi_{\alpha,k} \mathrm{e}^{-2\pi \mathrm{i} \epsilon_{\alpha,k} t} \phi_{\alpha,k}(x),\end{aligned} \tag{55}$$

calculate the expectation value $\langle x(t) \rangle$ of position as a function of time (see Appendix C), and obtain

$$\langle x(t) \rangle = \int_{-\infty}^{+\infty} dx\, x |\psi(x,t)|^2 = v_\infty t + o(t), \tag{56}$$

with

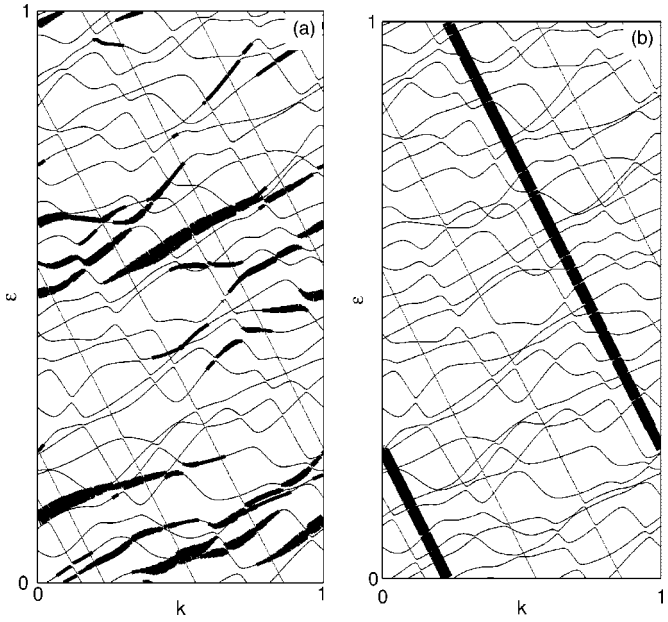

FIG. 8. Quasienergy band spectrum of the minimal ratchet model at $h^{-1}=32$. The linewidth encodes the overlap $|\langle \phi_{\alpha,k} | \psi \rangle|^2$ of the corresponding Floquet state $|\phi_{\alpha,k}\rangle$ with an initial wave packet $|\psi\rangle$. In (a) this wave packet is a coherent state located in the chaotic part of the phase space of a single unit cell; in (b) it is concentrated on a torus inside the major regular island [cf. Fig. 6(a)].

$$v_\infty = \int_0^1 dk \sum_{\alpha} |\psi_{\alpha,k}|^2 v_{\alpha,k}. \tag{57}$$

Consider now a wave packet localized initially within a single unit cell and, inside this unit cell, on one of the invariant sets of the classical dynamics. Then the weights $|\psi_{\alpha,k}|^2$ are approximately homogeneous in k but concentrated on the diabatic bands corresponding to the supporting invariant set. This is illustrated in Fig. 8. Consequently, the asymptotic velocity is an average over the corresponding band slopes. For example, for a wave packet started inside the chaotic sea we expect a value close to the classical chaotic transport velocity because this is the average slope of the chaotic bands; see Eq. (43). We confirm this semiclassical result in Fig. 9, where the average position of two chaotic wave packets is shown over a large time interval and for two different values of $N=h^{-1}$. In agreement with Eq. (56), we observe a linear dependence on time with very small fluctuations, i.e., asymptotically there is indeed directed ballistic quantum transport. The precise value of the velocity depends on the initial conditions but these fluctuations decrease with decreasing h and the average approaches the classical transport velocity. Typically the quantum velocity for a semiclassical chaotic wave packet is slightly above the classical value. This is a consequence of the hierarchical phase-space regions around the embedded islands which communicate with the main chaotic sea only via leaky cantori. Depending on h, quantum transitions across some of these cantori are possible only by tunneling, i.e., they are almost blocked. Therefore the part of the chaotic component enclosed by these cantori effectively belongs to the regular island [40] and, according

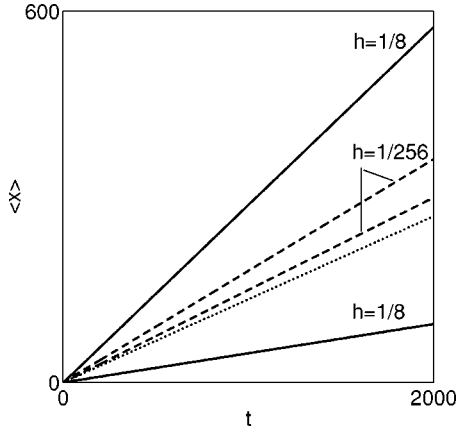

FIG. 9. Position vs time for wave packets initialized as coherent states inside the chaotic part of the phase space of the minimal ratchet model Eq. (31). Two different values of h and two different initial conditions are used. The dotted line shows the classical chaotic transport velocity.

to the sum rule (21), this enhanced island size is compensated by a correspondingly larger chaotic transport velocity.

2. Dynamical tunneling

On first sight it may surprise that the division of classical phase space into invariant sets can influence the long-time quantum dynamics. After all, classically impenetrable barriers can be crossed in quantum dynamics by tunneling. Tunneling is known best for the case of energetic barriers, e.g., in a double-well potential. Dynamical tunneling is the generalization of this phenomenon to barriers in phase space [41] and was recently demonstrated experimentally [42,43]. If in quantum dynamics no strict barriers exist, the wave packet should explore the entire accessible phase space for sufficiently long time and consequently directed transport should vanish, at least on average. We have seen in the previous section that this is not the case. So what is the role of tunneling in Hamiltonian ratchets?

To answer this question we consider a wave packet that is initially prepared inside the regular island within the unit cell $n_x=0$. Classically, such an initial distribution is simply transported along the chain of regular islands with a velocity corresponding to the winding number w_r, i.e., $P_r(x+w_r t,t)=P_r(x,t=0)$. This property is conserved in the quantum dynamics if we neglect the narrow avoided crossings in the band spectrum which account for the difference between adiabatic and diabatic bands. Let us demonstrate this for the regular island in our minimal model which has winding number $w_r=-1$. The diabatic regular bands are straight lines with slope w_r, i.e.,

$$\epsilon_{r,k}=\epsilon_{r,0}+w_r k. \tag{58}$$

As illustrated in Fig. 8(b), a localized initial wave packet can be constructed from such a band by a uniform superposition of all states

$$\Psi(x,t=0)=\int_0^1 dk\ \phi_{r,k}(x). \tag{59}$$

We restrict attention to times that are a multiple of the period μ_r of the central orbit inside the island. Then $w_r t$ is an integer which indicates one particular unit cell. We measure x relative to that unit cell and find for the wave packet

$$\begin{aligned}\Psi(x+w_r t,t)&=\int_0^1 dk\,\exp(-2\pi i\epsilon_{r,k}t)\phi_{r,k}(x+w_r t)\\&=\int_0^1 dk\,\exp[2\pi i(kw_r-\epsilon_{r,k})t]\phi_{r,k}(x)\\&=\exp(-2\pi i\epsilon_{r,0}t)\Psi(x,0).\end{aligned} \tag{60}$$

This shows that the wave packet is indeed transported like the corresponding classical distribution. It has the asymptotic velocity w_r and does not show any spreading, i.e., there is no signature of dynamical tunneling within the approximation of diabatic bands.

We conclude that tunneling out of an island in classical phase space is encoded in the avoided crossings between the regular and the chaotic bands. These avoided crossings show up in the regular bands as deviations from the straight line $\epsilon_{r,0}+\omega_r k$. Close to an avoided crossing the regular bands are bent toward the chaotic bands, i.e., the actual slope is k dependent and slightly smaller than w_r. Using this qualitative information about the shape of the regular bands we can make a prediction for the shape of the wave packet at very large times $t\to\infty$. In this regime the wave packet can be calculated from Eq. (55) in stationary-phase approximation. We find

$$\begin{aligned}\Psi(X+x,t)&=\int_0^1 dk\,\exp[2\pi i(kX-\epsilon_{r,k}t)]\phi_{r,k}(x)\\&=\sum_{\epsilon'_{r,k}=X/t}\sqrt{i/|\epsilon''_{r,k}t|}\exp(2\pi i[k\epsilon'_{r,k}-\epsilon_{r,k}]t)\phi_{r,k}(x).\end{aligned} \tag{61}$$

We have again decomposed the position into a large integer X denoting the unit cell and the remaining fraction $0<x<1$. $\phi_{r,k}(x)$ is considered a slowly varying prefactor of the rapidly oscillating phase. The points of stationary phase in Eq. (61) select the Bloch states whose superposition yields the wave packet at time t and position X. It is no surprise that these are exactly the points for which the slope of the band corresponds to the velocity X/t. Due to avoided crossings, the actual slope of the regular bands is smaller than w_r. Hence for the transition to the unit cell $X=w_r t$ where all classical probability is concentrated, no points of stationary phase with real k exist: To leading order this process is forbidden in quantum mechanics. There might be complex solutions of the equation $\epsilon'_{r,k}=w_r$, but then the exponent in Eq. (61) has a real part and the contribution will be exponentially small in t, which is indeed observed in Fig. 10(b). The main part of the wave packet is concentrated not in the "classical" unit cell but rather at positions for which real points of stationary phase exist in Eq. (61). These correspond to veloci-

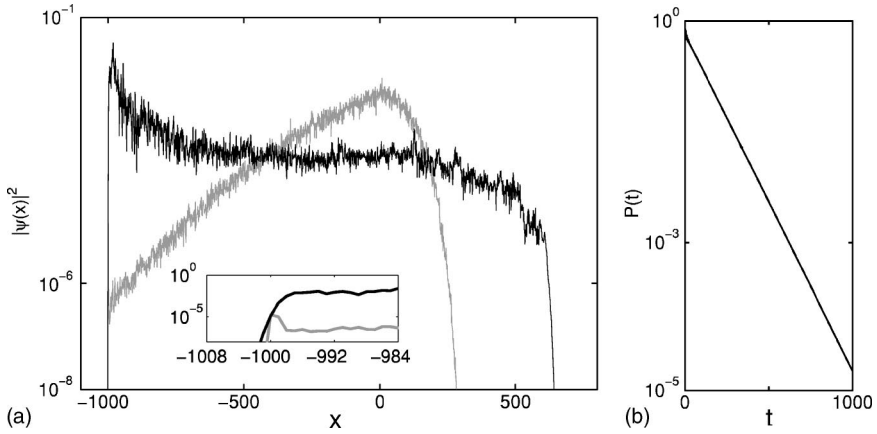

FIG. 10. (a) Black line: Wave packet prepared in the regular island of the unit cell $x=0$ and propagated to time $t=1000$ in the minimal ratchet model Eq. (31) with $h^{-1}=16$. The classical probability would be restricted to the unit cell $x=-1000$, while the quantum wave packet has tunneled out of this "classical" unit cell and starts spreading. However, there is a large peak lagging slightly behind the classically expected position. Gray line: Same for irrational $h^{-1}=16+\sigma$. In this case the Floquet operator has no spatial periodicity. The part of the wave packet outside the classical unit cell localizes and develops an asymmetric envelope with approximately exponential tails. Inset: The probability to remain inside the classically expected unit cell $x=-1000$ is the same for rational and irrational h. (b) Due to dynamical tunneling the quantum probability in this "classical" unit cell decays exponentially as a function of time. With respect to this decay the periodic model with $h^{-1}=16$ is almost indistinguishable from the aperiodic model with irrational $h^{-1}=16+\sigma$.

ties distributed narrowly around a value slightly below the classical velocity. Due to this dispersion in the velocities, induced by avoided crossings, the wave packet will spread ballistically in time and will be peaked behind the classically expected position [Fig. 10(a)].

For a wave packet initially prepared in the chaotic part of a unit cell the influence of tunneling is much less pronounced (not shown). Although the narrow avoided crossings with regular bands do modify the chaotic bands as well, the existence of points of stationary phase in an expansion similar to Eq. (61) is unaffected: due to the wide avoided crossings between themselves, the chaotic states have a large variation in their velocities around the classical value anyway.

We have thus identified the role of tunneling in Hamiltonian ratchets. It leads to avoided crossings between regular and chaotic states (or between regular states with different winding numbers). In the dynamics of initially localized wave packets tunneling shows up mainly in the evolution of regular states, which slightly lag behind the position expected from classical considerations. We stress again that tunneling is not able to hinder directed ballistic transport of such wave packets even for infinite time.

An interesting and important special case are systems with a symmetry-related pair of countermoving regular islands like the kicked rotor in the presence of accelerator modes. Dynamical tunneling between such island pairs was demonstrated experimentally [42,43]. It is crucial to understand the difference between our argumentation above and this situation. First we note that a pair of symmetry-related islands is *not* analogous to a symmetric double-well potential. In the latter case all eigenstates are superpositions of left and right. Below the barrier top, their eigenenergies form quasidegenerate doublets and thus contribute to tunneling. In the case of countermoving islands this applies only to the vicinity of avoided crossings between the corresponding bands where indeed they form a doublet. Away from these isolated and semiclassically small regions in k space the bands are approximately straight lines but *with opposite slopes*, i.e., there is no systematic degeneracy. In this paper we consider wave packets initially localized inside one unit cell. In k space such a wave packet is extended. Therefore its weight in the vicinity of avoided crossings, where it contributes to tunneling, is negligible. By contrast, in the experiments mentioned above the wave packets extend initially over many unit cells. Therefore, in k space they may well be concentrated right at avoided crossings. Then, and only then, dynamical tunneling is the expected consequence.

D. Quantum transport in the presence of disorder

In this last section we will describe some modifications of the quantum transport in a situation, when the exact quantum periodicity is destroyed by weak static disorder. As explained above in Sec. III A this can be realized easily within our minimal ratchet model by choosing an irrational value of h. In this case the Bloch theorem does not apply any more and, on a large scale, we expect dynamical localization of wave packets and eigenstates. The properties of the eigenstates and in particular the failure of the semiclassical eigenfunction hypothesis in this case have been studied in [21]. We will here concentrate on the evolution of wave packets in the presence of disorder. In Fig. 10 (gray line) we display the shape of a wave packet which was initialized in the regular island of unit cell $X=0$ at time $t=1000$. Initially the wave packet follows the classical evolution, i.e., it is transported at velocity $v=-1$ and loses probability due to tunneling. The process of tunneling out of the island is essentially the same as in the case of a periodic system with rational h. This is demonstrated by Fig. 10(b) and also by the inset of Fig. 10(a), where one can see that the probability remaining inside the classical unit cell is the same for both systems. However, the fate of the probability which has tunneled out of the

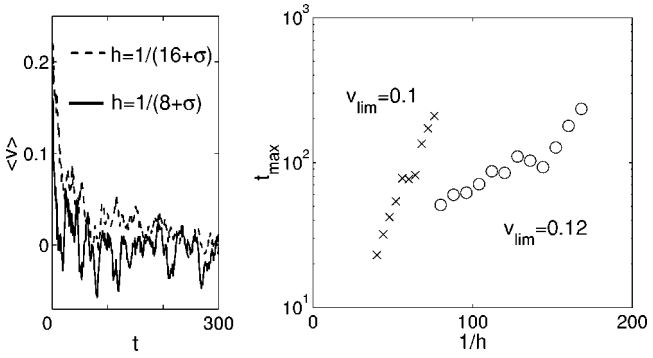

FIG. 11. (Left) Averaged velocity expectation values of wave packets initialized in the classically chaotic region at $(x_0,p_0)=(0,0.25\pm0.05)$. Beyond t_{loc}, the velocity oscillates around zero. (Right) Time $t_{\max}$ at which the averaged velocity expectation value falls short of a given limit under variation of h. For numerical reason, we chose two different values for v_{lim}.

island is entirely different from the periodic case. We see in Fig. 10(a) that the wave packet develops exponential tails which are characteristic of localization. Unlike the periodic case, the maximum of the wave packet is not close to the classical expectation but rather close to the origin, i.e., the disorder prevents quantum transport despite the underlying classical ratchet mechanism. The latter is manifest, however, in the asymmetric shape of the wave packet which has a much longer tail in the direction of classical transport.

Similarly, disorder does also affect wave packets that are initialized in the chaotic sea. Figure 11(a) shows the velocity expectation value for such a wave packet at two different values of the effective Planck's constant h. There is an initial period when $\langle v\rangle \sim v_{\mathrm{ch}}$, but then the velocity drops to zero because the wave packet tunnels into the island and finally occupies the whole available phase space. The time for this process is expected to scale as $t\sim e^{c/h}$ [44]. As Fig. 11(b) shows, this is also the time scale for which the quantum ratchet shows transport in the presence of disorder. This maximum ratchet operation time $t_{\max}$ can be defined as the time at which the velocity of a wave packet falls below a certain threshold. In Fig. 11(b) $\log_{10} t_{\max}$ is seen to depend approximately linearly on h^{-1}. Hence, in the deep semiclassical regime the quantum ratchet can work over an exponentially long time even in the presence of static disorder.

IV. DISCUSSION

The study of ratchets has largely been motivated by the interest in the physical principles of intracellular transport. Motor molecules, driven by chemical energy, are moving along chain molecules whose length is of the order of the cell size, and which consist of millions of units concatenated in a highly ordered manner, resembling the crystal order encountered in inorganic solids. It is therefore natural to model them as one-dimensional, infinitely extended potentials with exact spatial translation invariance, but with reflection symmetry manifestly broken to define a preferred direction of transport.

While the breaking of mirror symmetry is crucial to obtain directed transport, the role of translation invariance appears circumstantial, at most of heuristic importance for the theoretical description. Translation invariance has been indispensable, however, in order to achieve first analytical and numerical results on directed transport in ratchets. In the present context of Hamiltonian systems, it allowed us to show that directed transport comes about by counterpropagating phase-space flows within regular and chaotic components of systems with a mixed phase space. Moreover, quantum ratchets are obtained by quantizing Hamiltonian ratchets in the framework of Bloch theory; they exhibit transport at similar rates as their classical counterparts, at least in the semiclassical regime.

Real systems showing directed transport, biological or physical, though, break translation invariance in various ways and to various degrees, the only exception being systems where the spatial coordinate is cyclic, as in biological "rotation motors" or pumping devices in a closed configuration [45]. In the following we discuss a number of typical deviations from spatial periodicity and their consequences for transport. Since quantum systems are far more sensitive to the presence or absence of symmetries than classical ones, the question concerning imperfections of translation invariance becomes even more crucial on the quantum level.

Experimental realizations of Hamiltonian ratchets, as in optical lattices or in solid-state devices, always show a certain amount of *disorder*, in the form of small stochastic differences between the unit cells. Classically, smooth spatial disorder, if it is not too strong, will not completely disrupt the phase-space structures underlying transport on short time scales; thus it has only a minor effect on transport [46]. For long times, however, we expect that transport is destroyed. In extended quantum systems arbitrarily weak randomness in the potential immediately leads to localization. As we show in Sec. III D, even a type of disorder that is invisible in the classical dynamics entails a breakdown of quantum transport on a time scale proportional to the localization length. It should be kept in mind, however, that localization as a quantum coherence effect is counteracted, in turn, by incoherent processes caused by the unavoidable coupling to ambient degrees of freedom, or similarly by a "noisy" driving that breaks *temporal* periodicity. While it is well known that in this way, incoherence partially restores diffusive transport in systems with dynamical localization [47], its effects on *directed* transport remain to be explored.

The presence of a *spatially homogeneous force* breaks translational invariance in a more controlled yet radical manner. Rather than forming an unavoidable nuisance, it may be imposed intentionally to extract work from a ratchet. Moreover, it allows us to define a *stall force* as the external bias just sufficient to bring transport to a standstill [48], and to ascribe an efficiency to ratchets. In contrast to disorder, a finite mean potential gradient forms a perturbation of unbounded amplitude, and thus radically changes the structure of the classical ratchet phase space. Still, as explained in Sec. II F, directed regular transport reacts smoothly on an external bias, i.e., it requires a gradient of the order of those present in the original periodic potential to be completely suppressed. On the quantum level, additional complications arise in that eigenstates become metastable and eigenenergies correspondingly complex. This situation can be handled in a

framework similar to scattering theory [49]. Its application to ratchets is under way.

Finally, in most physical setups, transport takes place between two "terminals," typically modeled as electron reservoirs. This amounts to confining the ratchet proper to a finite section of space—yet another elementary way to break translational symmetry. Taking it into account would allow one to make contact with a different, but closely related paradigm of directed transport: *Pumps* are devices that channel a well-defined amount of charge, mass, etc., per cycle of an applied force from one terminal to the other [50,51]. Obviously, pumps can be considered as ratchets reduced to a finite number of unit cells, or conversely, ratchets could be constructed by concatenating an infinite number of pumps or equivalently by closing the pumping circuit. The only difference lies in the kind of model usually studied in these respective contexts, namely, fast drivings resulting in a chaotic dynamics in one case, slowly driven potential wells that resemble peristaltic pumps in the other [50]. But this is an artificial distinction: It has been shown recently that driven chaotic scattering systems, employed as pumps, also generate directed transport if all relevant binary symmetries are broken [52].

In order to study ratchets as realistic devices clamped between reservoirs at given temperatures and chemical potentials, however, another crucial building block is missing, a quantum statistical theory of transport under strong time-dependent driving far from equilibrium. For first approaches to this problem from the points of view of quantum scattering and quantum transport theory; see Refs. [53,45], respectively.

ACKNOWLEDGMENTS

We thank Marc-Felix Otto for his contribution to the project and in particular for the numerical data underlying Figs. 7–11. We benefited from discussions with D. Cohen, S. Fishman, S. Flach, P. Hänggi, M. Holthaus, P. Reimann, and O. Yevtushenko. T.D. acknowledges the hospitality enjoyed during stays at MPI für Physik komplexer Systeme (Dresden), MPI für Strömungsforschung (Göttingen), Universität Kaiserslautern, Centro Internacional de Ciencias (Cuernavaca), Weizmann Institute of Science (Rehovot), and Technion–Israel Institute of Technology (Haifa). Moreover, T.D. acknowledges financial support by the Volkswagen Foundation (Project No. I/78235), by the Weizmann Institute, by Colciencias (Project No. 310223), and by Dirección Nacional de Investigación (DINAIN, Project No. DI00C1255) and División de Investigación, Sede Bogotá (DIB, Project No. 803684) of Universidad Nacional de Colombia.

APPENDIX A: CHANGE OF MEAN MOMENTUM OF A KAM TORUS

In this appendix we consider a noncontractible KAM torus that can be specified by the functional dependence of the momentum on position and time $p(\xi,t)$. Note that the existence of such a function is an assumption which simplifies our reasoning.

We consider the average of the function $p(\xi,t)$ along the torus and replace the integral representation of this quantity, Eq. (25), by a Riemann sum over $N\to\infty$ discrete points $\xi_n = n/N$, $p_n = p(\xi_n,\tau)$,

$$\bar{p}(\tau) \approx \sum_{n=1}^{N} (\xi_{n+1} - \xi_n) p_n. \tag{A1}$$

Similarly we introduce a discrete time increment $\delta\tau$ and find that the N phase-space points (ξ_n, p_n, τ) in Eq. (A1) evolve to $(\tilde{\xi}_n, \tilde{p}_n, \tau+\delta\tau)$ with

$$\tilde{\xi}_n = \xi_n + p_n \delta\tau, \quad \tilde{p}_n = p_n - V'(\xi_n,\tau)\delta\tau. \tag{A2}$$

Now we use these new points to discretize the integral representing $\bar{p}(\tau+\delta\tau)$. In this way we obtain an expression for the time derivative of $\bar{p}$, which we evaluate to leading order in $\delta\tau$ and N^{-1} and then transform back to an integral. We obtain

$$\begin{aligned}
\frac{d}{d\tau}\bar{p}(\tau) &\approx \frac{1}{\delta\tau}\sum_{n=1}^{N} [(\tilde{\xi}_{n+1} - \tilde{\xi}_n)\tilde{p}_n - (\xi_{n+1} - \xi_n)p_n] \\
&= \frac{1}{\delta\tau}\sum_{n=1}^{N} \left\{ \left[\frac{1}{N} + (p_{n+1} - p_n)\delta\tau \right] \right. \\
&\quad \left. \times \left[p_n - V'(\xi_n,\tau)\delta\tau \right] - \frac{1}{N} p_n \right\} \\
&\approx \sum_{n=1}^{N} \left\{ -\frac{1}{N} V'(\xi_n,\tau) + (p_{n+1} - p_n) p_n \right\} \\
&\approx \frac{1}{N}\sum_{n=1}^{N} \{ -V'(\xi_n,\tau) + p_n p'(\xi_n,\tau) \} \\
&\approx \int_0^1 d\xi \left\{ -V'(\xi,\tau) + p(\xi,\tau)\frac{\partial}{\partial\xi} p(\xi,\tau) \right\} \\
&= \int_0^1 d\xi \left\{ -V'(\xi,\tau) + \frac{1}{2}\frac{\partial}{\partial\xi} p^2(\xi,\tau) \right\} \\
&= -\int_0^1 d\xi\, V'(\xi,\tau).
\end{aligned} \tag{A3}$$

For the last line we have used the periodicity of the function $p(\xi,\tau)$ with respect to ξ. By integration with respect to τ we find Eq. (26) which was the purpose of this appendix.

APPENDIX B: GENERALIZED FORM FACTOR FOR AN ISLAND CHAIN

In this appendix we derive Eq. (47). We consider the contribution to the form factor from one particular chain of regular islands r. If the winding number is $w_r^{\mathrm{cl}} = \nu_r/\mu_r$ then inside a unit cell this island chain consists of μ_r islands which are traversed in sequence. In the semiclassical limit, we associate (diabatic) bands with index α to the island chain. These

bands consist of straight-line segments with the slope $w_r^q = w_r^{\mathrm{cl}}$; cf. Eq. (41). The segments are connected such that the diabatic band as a whole is periodic in ϵ and k, with periods ν_r and μ_r, respectively. It is easy to see that for a given value of k there are μ_r equidistant segments (values of the quasienergy) pertaining to the same diabatic band α. Semiclassically, the number of states associated with the island chain for given k is approximately $f_r N$ where f_r is the fraction of the phase space occupied by the island chain as a whole and $N = h^{-1}$ is the total number of bands. It follows that the number of complete diabatic bands associated with the island is $f_r N/\mu_r$.

To integrate over a diabatic band consisting of many straight segments it is convenient to consider instead an extended Brillouin zone in which the band corresponds to a single straight line

$$\epsilon_{r,\alpha,k} = \left(\epsilon_{r,\alpha,0} + \frac{\nu_r}{\mu_r}k\right) \mod 1, \quad k \in [0,\mu_r). \tag{B1}$$

In this way we can perform the k integration in Eq. (45) and find

$$\begin{aligned} u_\alpha(n_x,m_t) &= \int_0^{\mu_r} dk\, e^{(2\pi i\{kn_x - [\epsilon_{r,\alpha,0} + (\nu_r/\mu_r)k]m_t\})} \\ &= \mu_r e^{-2\pi i \epsilon_{r,\alpha,0} m t} \int_0^1 d\kappa\, e^{2\pi i(\mu_r n_x - \nu_r m_t)\kappa} \\ &= \mu_r e^{-2\pi i \epsilon_{r,\alpha,0} m_t} \delta_{\mu_r n x - \nu_r m_t}. \end{aligned} \tag{B2}$$

For the contribution of the island chain r to the form factor we have now

$$K_r(n_x,m_t) = \frac{1}{N} \times \left\langle \left| \sum_{\alpha=1}^{N f_r/\mu_r} \mu_r e^{-2\pi i \epsilon_{r,\alpha,0} m_t} \delta_{\mu_r n_x - \nu_r m_t} \right|^2 \right\rangle, \tag{B3}$$

i.e., we have to perform a sum over quasienergies at fixed Bloch number $k=0$ which can be done in the same way as for the spectrum of eigenenergies pertaining to regular states of an autonomous system [54,55]. We assume the dynamics within the island to deviate sufficiently from harmonic vibrations around its central orbit. Then the spectrum of quasienergies $\epsilon_{r,\alpha,0}$ will not be equidistant and the phases in Eq. (B3) from different α can be assumed uncorrelated in the semiclassical limit. This allows us to replace $|\Sigma_\alpha \cdots|^2$ by the number of terms in the sum, which finally yields Eq. (47).

APPENDIX C: WAVE PACKET TRANSPORT

We compute the average position of a wave packet $\psi(x,t)$ for long time $t \gg 1$. First we write the wave packet as a superposition of Floquet eigenstates $\phi_{\alpha,k}(x)$ with quasienergy $\epsilon_{\alpha,k}$,

$$\begin{aligned} \psi(x,t) &= \sum_\alpha \int_0^1 dk\, \psi_{\alpha,k}(t)\phi_{\alpha,k}(x) \\ &= \sum_\alpha \int_0^1 dk\, \psi_{\alpha,k} e^{-2\pi i \epsilon_{\alpha,k} t} \phi_{\alpha,k}(x), \end{aligned} \tag{C1}$$

where

$$\psi_{\alpha,k} = \int_{-\infty}^{+\infty} dx\, \phi^*_{\alpha,k}(x)\psi(x,t=0). \tag{C2}$$

The integral representing the expectation value of $\hat{x}$ for the wave packet (C1) can be split into two contributions ξ, X corresponding to length scales within a unit cell and over many unit cells, respectively,

$$\begin{aligned} x(t) &= \int_{-\infty}^{+\infty} dx\, x|\psi(x,t)|^2 = \int_0^1 dx \sum_{n=-\infty}^{+\infty} (x+n)|\psi(x+n,t)|^2 \\ &= \xi(t) + X(t). \end{aligned} \tag{C3}$$

Naturally, the contribution from the dynamics inside the unit cells is bounded from above by the size of the unit cell

$$\xi(t) = \int_0^1 dx\, x \sum_{n=-\infty}^{+\infty} |\psi(x+n,t)|^2 \leqslant \int_0^1 dx \sum_{n=-\infty}^{+\infty} |\psi(x+n,t)|^2 = 1 \tag{C4}$$

(the last equality expresses the normalization of the wave packet). Therefore ξ is irrelevant for directed ballistic transport.

Evaluating the term that describes the wave packet on large scales, we use the Bloch theorem to switch from position representation to the conjugate variable k, where a spatial shift corresponds to differentiation. We have

$$\begin{aligned} n\psi(x+n,t) &= n\sum_\alpha \int_0^1 dk\, \psi_{\alpha,k}(t)\phi_{\alpha,k}(x+n) \\ &= \sum_\alpha \int_0^1 dk\, \psi_{\alpha,k}(t)\phi_{\alpha,k}(x) n e^{2\pi i k n} \\ &= \sum_\alpha \int_0^1 dk\, \psi_{\alpha,k}(t)\phi_{\alpha,k}(x) \frac{d}{dk}\frac{e^{2\pi i k n}}{2\pi i} \\ &= -\sum_\alpha \int_0^1 dk \frac{e^{2\pi i k n}}{2\pi i}\frac{d}{dk}\psi_{\alpha,k}(t)\phi_{\alpha,k}(x). \end{aligned}$$

The last line follows from partial integration and the periodicity in k of $e^{2\pi i k n}\psi_{\alpha,k}(t)\phi_{\alpha,k}(x)$. Inserting this into

$$X(t) = \int_0^1 dx \sum_{n=-\infty}^{+\infty} n|\psi(x+n,t)|^2$$

and decomposing also the complex conjugate $\psi^*(x+n,t)$ into Floquet states, we find

$$X(t) = -\int_0^1 dx \sum_{n=-\infty}^{+\infty} \sum_{\alpha,\alpha'} \int_0^1 dk \int_0^1 dk' \frac{e^{2\pi i(k-k')n}}{2\pi i}$$

$$\times \psi^*_{\alpha',k'}(t)\phi^*_{\alpha',k'}(x)\frac{d}{dk}\psi_{\alpha,k}(t)\phi_{\alpha,k}(x)$$

$$= -\frac{1}{2\pi i}\int_0^1 dx \sum_{\alpha,\alpha'} \int_0^1 dk$$

$$\times \psi^*_{\alpha',k}(t)\phi^*_{\alpha',k}(x)\frac{d}{dk}\psi_{\alpha,k}e^{-2\pi i\epsilon_{\alpha,k}t}\phi_{\alpha,k}(x).$$

The last line follows here from Poisson summation over n. In this expression d/dk acts on a product of three terms, but as $t\to\infty$ the dominant contribution comes from the derivative of the exponential. Neglecting the other two terms which are bounded, and using the orthonormalization of Floquet states we finally obtain Eqs. (56) and (57).

For higher moments of the spatial distribution the argument can be repeated and an analogous result is obtained

$$\langle [x - x(t)]^m \rangle = t^m \sum_\alpha \int_0^1 dk |\psi_{\alpha,k}|^2 \left(\frac{d\epsilon\alpha,k}{dk}\right)^m + O(t^{m-1}). \quad \text{(C5)}$$

[1] S. Flach, O. Yevtushenko, and Y. Zolotaryuk, Phys. Rev. Lett. **84**, 2358 (2000).
[2] T. Dittrich, R. Ketzmerick, M. F. Otto, and H. Schanz, Ann. Phys. (Leipzig) **9**, 755 (2000).
[3] H. Schanz, M. F. Otto, R. Ketzmerick, and T. Dittrich, Phys. Rev. Lett. **87**, 070601 (2001).
[4] S. Denisov and S. Flach, Phys. Rev. E **64**, 056236 (2001).
[5] S. Denisov *et al.*, Physica D **170**, 131 (2002).
[6] P. Jung, J. G. Kissner, and P. Hänggi, Phys. Rev. Lett. **76**, 3436 (1996).
[7] J. L. Mateos, Phys. Rev. Lett. **84**, 258 (2000).
[8] J. L. Mateos, Physica A **325**, 92 (2003).
[9] R. P. Feynman, R. B. Leighton, and M. Sands, *The Feynman Lectures on Physics* (Addison-Wesley, Reading, MA, 1966), Vol. 1, Chap. 46.
[10] F. Jülicher, A. Ajdari, and J. Prost, Rev. Mod. Phys. **69**, 1269 (1997).
[11] P. Reimann, Phys. Rep. **361**, 57 (2002).
[12] R. D. Astumian and P. Hänggi, Phys. Today **55**, 33 (2002).
[13] T. S. Monteiro *et al.*, Phys. Rev. Lett. **89**, 194102 (2002).
[14] N. A. C. Hutchings *et al.*, Phys. Rev. E **70**, 036205 (2004).
[15] I. Goychuk and P. Hänggi, *Directed current without dissipation: re-incarnation of a Maxwell-Loschmidt-demon*, Lecture Notes Physics Vol. 557, (Springer, Berlin, 2000), p. 7.
[16] I. Goychuk and P. Hänggi, J. Phys. Chem. B **105**, 6642 (2001).
[17] J. B. Gong and P. Brumer, Phys. Rev. E **70**, 016202 (2004).
[18] D. del Castillo-Negrete, Phys. Fluids **10**, 576 (1998).
[19] H. Linke *et al.*, Science **286**, 2314 (1999).
[20] E. M. Hohberger *et al.*, Appl. Phys. Lett. **78**, 2905 (2001).
[21] L. Hufnagel, R. Ketzmerick, M. F. Otto, and H. Schanz, Phys. Rev. Lett. **89**, 154101 (2002).
[22] In this paper all quantities are dimensionless. Distance and time are measured in units of the corresponding periods and the particle mass is set to unity. It follows that also velocity, momentum, energy, etc. are dimensionless.
[23] G. Casati and L. Molinari, Prog. Theor. Phys. Suppl. **98**, 285 (1989).
[24] E. Ott, *Chaos in Dynamical Systems* (Cambridge University Press, Cambridge, U.K., 1993).
[25] L. A. Bunimovich, Chaos **11**, 802 (2001).
[26] J. Malovrh and T. Prosen, J. Phys. A **35**, 2483 (2002).
[27] F. M. Izrailev, Phys. Rep. **196**, 299 (1990).
[28] F. L. Moore *et al.*, Phys. Rev. Lett. **75**, 4598 (1995).
[29] B. G. Klappauf *et al.*, Phys. Rev. Lett. **81**, 1203 (1998).
[30] H. Sambe, Phys. Rev. A **7**, 2203 (1973).
[31] I. C. Percival, J. Phys. B **6**, L229 (1973).
[32] M. V. Berry, J. Phys. A **10**, 2083 (1977).
[33] M. Hillery *et al.*, Phys. Rep. **106**, 121 (1984).
[34] A. R. Kolovsky, S. Miyazaki, and R. Graham, Phys. Rev. E **49**, 70 (1994).
[35] T. Dittrich, B. Mehlig, H. Schanz, and U. Smilansky, Phys. Rev. E **57**, 359 (1998).
[36] T. Dittrich, B. Mehlig, H. Schanz, and U. Smilansky, Chaos, Solitons Fractals **8**, 1205 (1997).
[37] J. H. Hannay and A. M. Ozorio de Almeida, J. Phys. A **17**, 3429 (1984).
[38] M. V. Berry, Proc. R. Soc. London, Ser. A **400**, 229 (1985).
[39] S. Müller *et al.*, Phys. Rev. Lett. **93**, 014103 (2004).
[40] R. Ketzmerick *et al.*, Phys. Rev. Lett. **85**, 1214 (2000); in the present work we neglect the existence of hierarchical states, but see this reference.
[41] M. J. Davis and E. J. Heller, J. Chem. Phys. **75**, 246 (1981).
[42] D. A. Steck, W. H. Oskay, and M. G. Raizen, Science **293**, 274 (2001).
[43] W. K. Hensinger *et al.*, Nature (London) **412**, 52 (2001).
[44] J. D. Hanson, E. Ott, and T. M. Antonsen, Phys. Rev. A **29**, 819 (1984).
[45] D. Cohen, Phys. Rev. B **68**, 155303 (2003).
[46] W. Acevedo, C. Pineda, and T. Dittrich, in *Nonlinear Dynamics and the Spatiotemporal Principles of Biology*, edited by F. Beck, M.-T. Hütt, and U. Lüttge, special issue of Nova Acta Leopold. **88**, 279 (2003).
[47] T. Dittrich and R. Graham, Ann. Phys. (N.Y.) **200**, 363 (1990).
[48] P. Reimann and P. Hänggi, Appl. Phys. A: Mater. Sci. Process. **75**, 169 (2002).
[49] M. Glück, A. R. Kolovsky, and H. J. Korsch, Phys. Rep. **366**, 103 (2002).
[50] P. W. Brouwer, Phys. Rev. B **58**, R10135 (1998).
[51] E. Akkermans *et al.*, Ann. Phys. (N.Y.) **284**, 10 (2000).
[52] T. Dittrich, M. Gutierrez, and G. Sinuco, Physica A **327**, 145 (2003).
[53] M. Moskalets and M. Büttiker, Phys. Rev. B **66**, 205320 (2002).
[54] M. V. Berry and M. Tabor, Proc. R. Soc. London, Ser. A **356**, 375 (1977).
[55] T. Dittrich, Phys. Rep. **271**, 267 (1996).